

AD-A058 465

PENNSYLVANIA STATE UNIV UNIVERSITY PARK APPLIED RESE--ETC F/8 11/10  
AN EXPERIMENTAL DETERMINATION OF THE DYNAMIC YOUNG'S MODULUS OF--ETC(U)  
DEC 76 V M MAZA

UNCLASSIFIED

ARL/PSU/TH-76-313

N00017-73-C-1418

NL

1 OF 1  
AD  
A058465



ADA 058465

AD No. \_\_\_\_\_  
DDC FILE COPY

**LEVEL** 11

12

6

AN EXPERIMENTAL DETERMINATION OF THE DYNAMIC  
YOUNG'S MODULUS OF SELECTED VISCOELASTIC MATERIALS

Victor M. Maza

Technical Memorandum  
File No. TM 76-313  
December 14, 1976  
Contract No. N00017-73-C-1418

Copy No. 16

DDC  
RECEIVED  
SEP 7 1978  
F

The Pennsylvania State University  
Institute for Science and Engineering  
APPLIED RESEARCH LABORATORY  
Post Office Box 30  
State College, PA 16801

APPROVED FOR PUBLIC RELEASE  
DISTRIBUTION UNLIMITED

NAVY DEPARTMENT

NAVAL SEA SYSTEMS COMMAND

78 08 31 040

UNCLASSIFIED

SECURITY CLASSIFICATION OF THIS PAGE (When Data Entered)

(14) ARL/PSU/TM-76-313

REPORT DOCUMENTATION PAGE		READ INSTRUCTIONS BEFORE COMPLETING FORM
1. REPORT NUMBER TM 76-313	2. GOVT ACCESSION NO.	3. RECIPIENT'S CATALOG NUMBER ⑨ Master's Thesis
4. TITLE (and Subtitle) ⑥ AN EXPERIMENTAL DETERMINATION OF THE DYNAMIC YOUNG'S MODULUS OF SELECTED VISCOELASTIC MATERIALS.		5. TYPE OF REPORT & PERIOD COVERED M.S. Thesis, August 1977
7. AUTHOR(s) ⑩ Victor M. Maza		6. PERFORMING ORG. REPORT NUMBER TM 76-313
9. PERFORMING ORGANIZATION NAME AND ADDRESS The Pennsylvania State University Applied Research Laboratory P. O. Box 30, State College, PA 16801		8. CONTRACT OR GRANT NUMBER(s) N00017-73-C-1418
11. CONTROLLING OFFICE NAME AND ADDRESS Naval Sea Systems Command Department of the Navy Washington, D. C. 20362		10. PROGRAM ELEMENT, PROJECT, TASK AREA & WORK UNIT NUMBERS ⑪ 14 Dec 76 ⑫ 77p.
14. MONITORING AGENCY NAME & ADDRESS (if different from Controlling Office)		12. REPORT DATE December 14, 1976
		13. NUMBER OF PAGES 74 pages & figures
		15. SECURITY CLASS. (of this report) Unclassified, Unlimited
		15a. DECLASSIFICATION/DOWNGRADING SCHEDULE
16. DISTRIBUTION STATEMENT (of this Report) Approved for public release, distribution unlimited, per NSSC (Naval Sea Systems Command), 4/4/77		
17. DISTRIBUTION STATEMENT (of the abstract entered in Block 20, if different from Report)		
18. SUPPLEMENTARY NOTES		
19. KEY WORDS (Continue on reverse side if necessary and identify by block number) materials elastomers viscoelasticity Young's modulus		
20. ABSTRACT (Continue on reverse side if necessary and identify by block number) Viscoelastic materials or elastomers are widely used to isolate transmission of vibrations. The elastic characteristics of these materials can be understood if the bulk, shear and Young's moduli are known. In this study, results of the dynamic characteristics of the Young's modulus over a wide range of frequencies were obtained for eight different elastomers. Samples of the different viscoelastic materials were attached to an oscillator and different vibratory frequencies were excited. Voltage and phase difference of the waves propagating along the elastomers were recorded.		

DD FORM 1 JAN 73 1473

EDITION OF 1 NOV 65 IS OBSOLETE

391007

UNCLASSIFIED

SECURITY CLASSIFICATION OF THIS PAGE (When Data Entered)

78 08 31 040

UNCLASSIFIED

SECURITY CLASSIFICATION OF THIS PAGE(When Data Entered)

20. ABSTRACT (Continued)

by means of a stereo pick-up and graphs of voltage versus distance and phase versus distance were drawn in order to obtain the attenuation constant and wavelength, respectively. With these values, the loss factor and the dynamic Young's modulus were obtained. The measurement frequency was limited by the attenuation constant which increases with frequency and by the noise of the system. The moduli are dependent upon frequency, temperature and the material. At a constant temperature of 28°C and at various frequencies, it was found that some of them show glass-like, and others show rubber-like properties. It was also found that the storage Young's modulus or real part of the modulus is of the order of  $1.8 \times 10^9$  Newtons/m<sup>2</sup> for polyester; of the order of  $10^8$  for polyurethane and synthetic rubber; and of the order of  $10^7$  for natural rubber neoprene. In addition, the loss factors were also measured.

ACCESSION for	
NTIS	White Section <input checked="" type="checkbox"/>
DDC	Buff Section <input type="checkbox"/>
UNANNO INDEX	<input type="checkbox"/>
JUST 101 101	
BY	
DISSEMINATION/AVAILABILITY CODES	
CINL	
A	

UNCLASSIFIED

SECURITY CLASSIFICATION OF THIS PAGE(When Data Entered)



#### ACKNOWLEDGMENTS

The author would like to express his sincere gratitude to Dr. Dennis W. Ricker for his assistance and guidance during the course of the research, and for his suggestions which were helpful in the preparation of this thesis.

This research was supported by the Applied Research Laboratory of The Pennsylvania State University under contract with the Naval Sea System Command.

## TABLE OF CONTENTS

	<u>Page</u>
ACKNOWLEDGEMENTS . . . . .	11
LIST OF TABLES . . . . .	iv
LIST OF FIGURES . . . . .	v
SYMBOLS . . . . .	vii
I. INTRODUCTION . . . . .	1
II. GENERAL BEHAVIOR OF VISCOELASTIC MATERIALS . . . . .	3
2.1 Historical Background and Generalities . . . . .	3
2.2 Stress-Strain Linear Relationships and Elasticity Modulus . . . . .	5
2.3 Stress-Strain Complex Relationships . . . . .	9
2.4 Mechanical Analogies of Viscoelastic Linear Behavior . . . . .	11
2.5 Wave Propagation in Long Rods; Young's Modulus and Loss Factor . . . . .	12
2.6 Frequency and Temperature Dependence . . . . .	14
III. EXPERIMENTAL SET-UP FOR TENSILE TEST . . . . .	18
3.1 Kuehl and Meyer Technique . . . . .	18
3.2 Nolle's Technique . . . . .	21
3.3 Characteristics of the Pick-up System . . . . .	23
3.4 Relation Between the Stereo Signal and the Longitudinal and Transverse Waves . . . . .	26
3.5 Materials Tested . . . . .	29
3.6 Experimental Problems . . . . .	32
IV. EXPERIMENTAL RESULTS . . . . .	36
4.1 Reduction and Interpretation of Data . . . . .	36
4.2 Young's Modulus and Loss Factor Results . . . . .	39
4.3 Error Considerations . . . . .	57
V. CONCLUSIONS . . . . .	58
5.1 Findings . . . . .	58
5.2 Analysis of Data . . . . .	58
5.3 Recommendations for Further Studies . . . . .	63
BIBLIOGRAPHY . . . . .	65

## LIST OF TABLES

<u>Table</u>	<u>Page</u>
5.1 Viscoelastic Properties of Various Elastomers . . . . .	59
5.2 Categorization of the Tested Materials at 28°C . . . . .	63

## LIST OF FIGURES

<u>Figure</u>	<u>Page</u>
2.1.1 Stress and Strain Sinusoidal Excitations . . . . .	4
2.2.1 Moduli of Linear Elastic Deformation	
a) Simple Shear . . . . .	7
b) Bulk Compression . . . . .	8
c) Plane Wave Compression . . . . .	8
d) Simple Extension . . . . .	8
e) Poisson's Ratio . . . . .	9
2.3.1 Vector Representation of Stress and Strain . . . . .	9
2.4.1 Maxwell and Voigt Simple Models of Linear Viscoelasticity . . . . .	12
2.6.1 Tobolsky Regions of Viscoelastic Behavior Based on Creep Experiments . . . . .	16
2.6.2 Behavior of Viscoelastic Moduli . . . . .	16
3.1.1 Apparatus to Test Longitudinal Wave Propagation; Technique of Kuehl and Meyer . . . . .	19
3.2.1 System of Triaxial Rulers . . . . .	22
3.2.2 Electronic Box-Diagram for Measurement of Wave Propagation on an Elastomer; Technique of Nolle . . . .	24
3.4.1 Schematic View of Groove Undulations in a Stereophonic Disc Phonograph Record . . . . .	27
3.4.2 Particle Motion for Longitudinal Wave . . . . .	27
3.4.3 Particle Motion for Transverse Waves . . . . .	27
3.4.4 Longitudinal and Transverse Signals on an Elastomer . .	28
3.4.5 Stylus on a Record Player Groove . . . . .	28
3.4.6 Vectorial Components of Longitudinal and Transverse Wave . . . . .	30
3.5.1 Elastomer Sample . . . . .	31
3.6.1 Measurement of Transverse Waves with Flexural Waves as a Disturbance . . . . .	33
3.6.2 Connections Between Shaker and Elastomer . . . . .	35



<u>Figure</u>	<u>Page</u>
4.1.1 Typical Phase Difference as a Function of Distance . . .	37
4.1.2 Typical Wave Pressure as a Function of Distance . . . .	38
4.1.3 Typical Attenuation Constant Versus Frequency . . . . .	40
4.2.1 Attenuation Constant for Castomold Polyester . . . . .	41
4.2.2 Storage and Loss Young's Modulus and Loss Factor for Castomold Polyester . . . . .	42
4.2.3 Attenuation Constant for EN-6 Polyurethane . . . . .	43
4.2.4 Storage and Loss Young's Modulus and Loss Factor for EN-6 Polyurethane . . . . .	44
4.2.5 Attenuation Constant for Hypalon H-862 . . . . .	45
4.2.6 Storage and Loss Young's Modulus and Loss Factor for Hypalon H-862 . . . . .	46
4.2.7 Attenuation Constant for PRC-1564 . . . . .	47
4.2.8 Storage and Loss Young's Modulus and Loss Factor for PRC-1564 . . . . .	48
4.2.9 Attenuation Constant for Butyl B-252 . . . . .	49
4.2.10 Storage and Loss Young's Modulus and Loss Factor for Butyl B-252 . . . . .	50
4.2.11 Attenuation Constant for Natural Rubber 33001 . . . . .	51
4.2.12 Storage and Loss Young's Modulus and Loss Factor for Natural Rubber 33001 . . . . .	52
4.2.13 Attenuation Constant for Neoprene 33003 . . . . .	53
4.2.14 Storage and Loss Young's Modulus and Loss Factor for Neoprene 33003 . . . . .	54
4.2.15 Attenuation Constant for PRC-1524 . . . . .	55
4.2.16 Storage and Loss Young's Modulus and Loss Factor for PRC-1524 . . . . .	56
5.1 Storage Modulus for Eight Viscoelastic Materials . . . . .	61
5.2 Loss Factor for Eight Viscoelastic Materials . . . . .	62

## SYMBOLS

$A_t$	transversal area
$c$	velocity of wave
$c_c$	compressional wave velocity
$c_f$	flexural wave velocity
$E$	real component of Young's modulus
$E^*$	complex component of Young's modulus
$E'$	storage Young's modulus
$E''$	loss Young's modulus
$F$	force
$f$	frequency
$G$	real component of shear modulus
$G^*$	complex component of shear modulus
$G'$	storage shear modulus
$G''$	loss shear modulus
$h$	width
$j$	imaginary unit $\sqrt{-1}$
$K$	real component of bulk modulus
$K^*$	complex component of bulk modulus
$K'$	storage bulk modulus
$K''$	loss bulk modulus
$k$	wave number
$l$	length
$\Delta l$	elongation
$M$	real component of plane wave modulus
$M^*$	complex component of plane wave modulus
$M'$	storage plane wave modulus

$M''$	loss plane wave modulus
$P, P_1$	pressure
$r$	loss parameter
$t$	width
$\Delta t$	transversal contraction
$V$	volume
$\Delta V$	volume contraction
$x, x_1$	distance along the elastomer
$\alpha$	attenuation constant
$\epsilon$	strain
$\epsilon_0$	maximum strain amplitude
$\theta$	angle of strain deformation
$\psi$	phase difference
$\eta$	loss factor
$\lambda$	wavelength of vibration
$\rho, \rho^*$	Poisson's ratio
$\rho$	density
$\sigma$	stress
$\sigma_0$	maximum stress amplitude
$\sigma'$	component of stress in phase with strain
$\sigma''$	component of stress out of phase with strain
$\omega$	frequency in radians

## CHAPTER I

### INTRODUCTION

Rubber and other viscoelastic materials otherwise referred to as elastomers are widely used as vibration isolators to reduce the transmission of vibratory forces or displacements. They are also used as vibration dampers, turning motion into heat in order to reduce the vibratory response of a system, especially near frequencies of resonance. They are good antivibration mountings, especially when isolating small machinery and mechanical devices.

Elastomers are utilized in many other applications, including underwater sound systems where they find use as sound reflectors, sonar domes, lining for test tanks and transducer windows.<sup>1</sup> In some cases, transmissibility of the material is important; in others, its absorption coefficient and its characteristic impedance take larger roles.

It is clear from the previous statements that the study of the characteristics of elastomers is of great importance. There exists a vast amount of literature pertaining to elastomers and studies concerning their different characteristics, including moduli of elasticity, absorption constant, loss factor, as well as their ability to transmit and reflect acoustic energy.

In order to completely characterize the engineering properties of an elastomer, it is important that the bulk, shear and Young's moduli be known. In this thesis, the complex Young's modulus of eight different elastomers is experimentally obtained over a wide



range of frequencies. This data, in conjunction with that obtained through an Applied Research Laboratory's grant to the Physics Department of the University of Texas will allow a complete characterization of these selected materials.

When elastomers are used as transducer windows, impedance matching with the water, together with material stiffness and losses are very important. The results of this thesis will provide needed data to aid in the selection of those materials best suited to these applications.

In Chapter II, the general stress-strain relations pertaining to elastomers are discussed. In addition, the relationships between the moduli and their dependence upon frequency and temperature are considered. Chapter III covers in detail experimental procedures and a discussion of the relative limits of various approaches is provided. The experimental results are presented in Chapter IV and interpretation of the data, conclusions and recommendations for further studies is covered in Chapter V.

## CHAPTER II

### GENERAL BEHAVIOR OF VISCOELASTIC MATERIALS

#### 2.1 Historical Background and Generalities

Over the years, an increasing number of studies related to the properties of different viscoelastic materials have been made. At first, studies were made of static characteristics and it was not until the early forties that important studies of dynamic characteristics were made at various laboratories and research centers.

Rubbers are capable of achieving large elastic deformations and are generally able to recover their original shape once the deforming stress is removed. In the early theories of elasticity, it was considered that the body returns to its original shape instantly; however, even if it seems that the rubber regained its original shape, there may still be some residual strain which will decay over a period of time. Observations were made of this phenomenon, and some time dependent effect relations were proposed by Boltzmann<sup>2</sup> in 1874. Some time before that, Gough<sup>3</sup> noticed that rubbers behave differently at different temperatures and that heat is generated when they are extended. This represented the beginning of the studies of the non-static behavior of rubber. These studies, together with previously developed static theories, provided the basis for the development of a vast amount of literature on the properties of viscoelastic materials.

The classical theory of elasticity formulated by Hooke<sup>4</sup> in 1678 states the relation of proportionality between stress and strain;

the stress being proportional to the strain but independent of the rate of strain. This relation holds for an ideal situation; the stress-strain behavior, however, is in general more complicated. When an elastomer is deformed, the stress needed to hold a constant strain will eventually diminish. This phenomenon is called stress relaxation. Similarly, when a constant stress is applied to an elastomer, it undergoes a strain which will increase or "creep" with time until breakage occurs. These two processes are time dependent. In the case of a sinusoidally varying stress, the resultant strain will also vary sinusoidally but with lagging phase as shown in Figure 2.1.1.

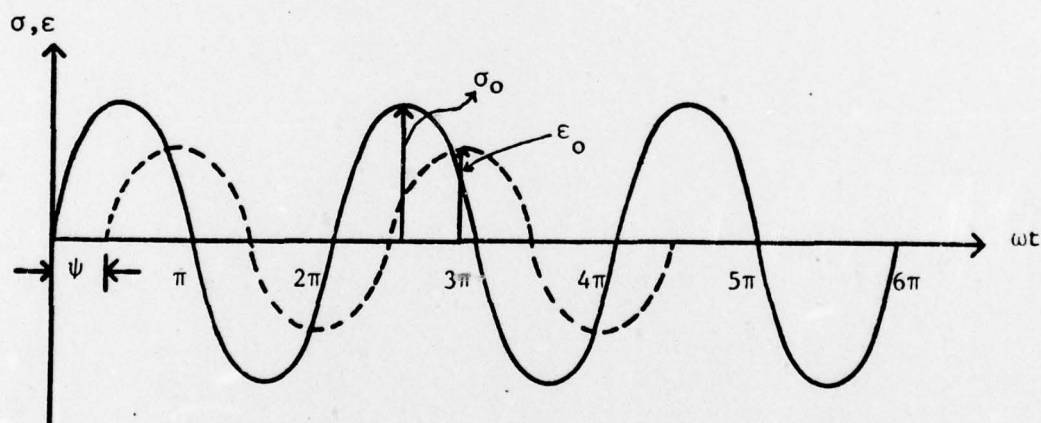


Figure 2.1.1. Stress and Strain Sinusoidal Excitations

Equations describing these curves are:

$$\sigma = \sigma_0 \sin \omega t \quad (2.1.1)$$

and

$$\epsilon = \epsilon_0 \sin (\omega t + \psi) \quad , \quad (2.1.2)$$

where  $\sigma$  and  $\sigma_0$  are the stress and the stress maximum amplitude,  $\epsilon$  and  $\epsilon_0$  are the strain and the strain maximum amplitude, and  $\psi$  is the phase difference.

In a viscous medium with an applied stress, the molecules are not all displaced at the same velocity. Some will displace faster than others, causing a drag on the slower ones with a resulting time dependent strain. If the medium were perfectly viscous, the resulting strain would be 90 degrees out of phase from a sinusoidally varying stress.

Elastomers are neither perfectly elastic nor viscous, but combine both effects. These materials are capable of absorbing great amounts of energy and, in order to discuss their dynamic behavior, it is necessary to consider both their elastic and their viscous properties.

The moduli of viscoelastic materials vary as a function of frequency and temperature and the effects are inversely related. They generally exhibit rubber-like properties at high temperatures or low frequencies and glass-like properties at lower temperatures or at high frequencies. An exact description of the stress-strain behavior of a given elastomer would generally involve a very complex nonlinear model. However, simplifications based on linear network theory have been shown to be accurate for small deformations.<sup>5</sup>

## 2.2 Stress-Strain Linear Relationships and Modulus of Elasticity

Two basic types of deformation may be experienced by a material



when a stress is applied to it; shear deformation which implies a change of shape without a change in volume, and bulk deformation which implies changes in volume but not in shape. Both are described<sup>6,10</sup> respectively by the shear modulus  $G$  and the bulk modulus  $K$  where:

$$G = \frac{F/A_t}{d (\tan \theta)} \quad (2.2.1)$$

and

$$K = \frac{P}{\Delta V/V} \quad , \quad (2.2.2)$$

where

$F$  = force applied on the body,

$A_t$  = area of the face transverse to the applied force,

$\theta$  = angle of strain deformation,

$P$  = pressure applied on the body,

and  $\Delta V, V$  = volume compression and volume of the body.

Other moduli, which involve both change in volume and shape are the plane wave modulus:

$$M = K + \frac{4}{3} G \quad , \quad (2.2.3)$$

which represents the ratio of stress to strain in a medium where the lateral dimensions are large compared to the longitudinal dimensions, and the Young's modulus:

$$E = \frac{9KG}{3K + G} \quad , \quad (2.2.4)$$

which is the ratio of longitudinal stress to longitudinal strain for a thin rod. Another equation describing it is:

$$E = 2(1 + \rho)G \quad , \quad (2.2.5)$$

where  $\rho$  is the ratio of Poisson, defined as the ratio of lateral strain to longitudinal strain for a thin rod, and it is equal to:

$$\rho = \frac{\Delta t/t}{\Delta l/l} \quad (2.2.6)$$

where

$\Delta t$  = contraction suffered by the rod,

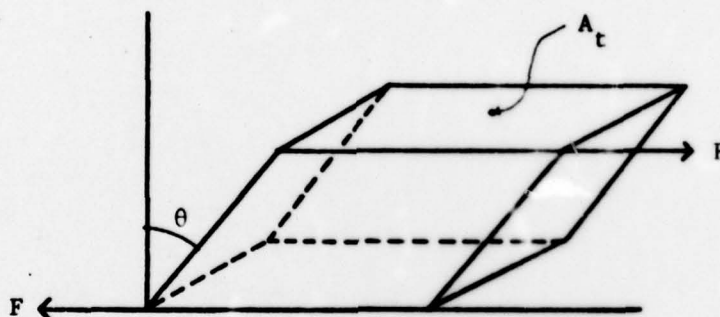
$t$  = width of the rod,

$\Delta l$  = elongation experience by the rod,

and  $l$  = length of the sample.

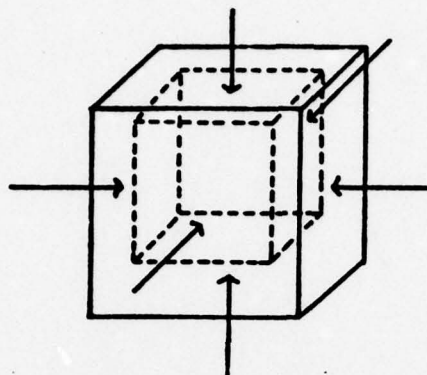
These basic types of deformation and the moduli describing them are basic tools for studying the static elastic characteristics of a material; however, when considering dynamic stress and strain, it is necessary to take into consideration the complex elastic moduli which are discussed in Section 2.3.

Figure 2.2.1 shows the basic deformation in elasticity and the equations related to them.



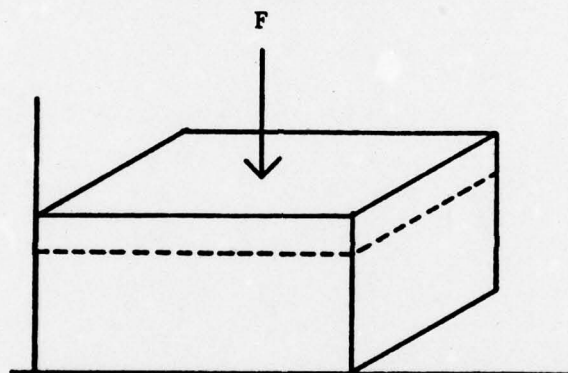
$$G = \frac{F/\Delta t}{d (\tan \theta)}$$

a) Simple Shear



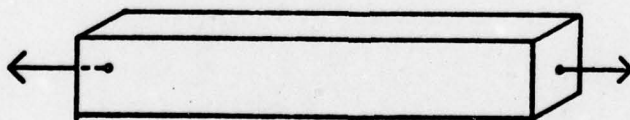
$$K = \frac{P}{\Delta V/V}$$

b) Bulk Compression



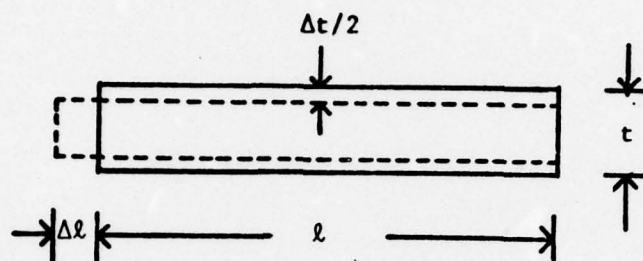
$$M = K + \frac{4}{3}G$$

c) Plane Wave Compression



$$E = \frac{9KG}{3K + G} = \frac{F/A}{\Delta l/l}$$

d) Simple Extension



$$\rho = \frac{\Delta t/t}{\Delta l/l}$$

e) Poisson's Ratio

Figure 2.2.1. (a through e) Moduli of Linear Elastic Deformation.

### 2.3 Stress-Strain Complex Relationships

When a sinusoidal stress is applied on a viscoelastic material, the resulting sinusoidal strain will lag the stress by a certain phase difference. The stress can be decomposed into two components, one in phase and another 90 degrees out of phase with strain as shown in Figure 2.3.1.

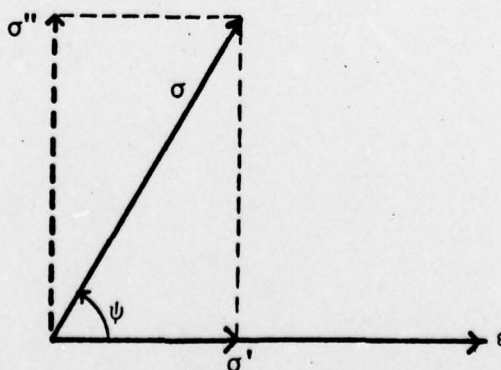


Figure 2.3.1. Vector Representation of Stress and Strain.



$\sigma$  = stress,

$\sigma'$  = component in phase with strain,

$\sigma''$  = component out of phase with strain,

$\epsilon$  = strain,

and  $\psi$  = phase difference between stress and strain,

where 
$$\tan \psi = \frac{\sigma''}{\sigma'} = \eta \quad (2.3.1)$$

and  $\eta$  is often called the loss factor.

The projection of the stress vector over the strain vector gives a component in phase with the strain, and the projection of the stress vector over another vector perpendicular to the strain, gives the component 90 degrees out of phase with respect to strain. The shear modulus of a body with a stress applied is the ratio of stress to strain produced:

$$G = \frac{\sigma}{\epsilon} \quad (2.3.2)$$

This ratio, when considering both the in-phase and out-of-phase stress components, becomes a complex quantity represented by:

$$G^* = G' + jG'' \quad (2.3.3)$$

where

$$G' = \frac{\sigma'}{\epsilon} \quad (2.3.4)$$

and

$$G'' = \frac{\sigma''}{\epsilon} \quad (2.3.5)$$

These ratios are called the storage modulus and the loss modulus, respectively.

The loss factor can now be defined as:

$$\eta = \frac{G''}{G'} \quad (2.3.6)$$

where  $\tan \psi = \eta$  as previously defined by Equation (2.3.1).

Similarly, other moduli are represented by their storage and their loss modulus as follows:

$$K^* = K' + jK'' \quad , \quad (2.3.7)$$

$$E^* = E' + jE'' \quad (2.3.8)$$

and  $M^* = M' + jM'' \quad (2.3.9)$

where the loss factors of each moduli are represented by:

$$\eta_K = \frac{K''}{K'} \quad , \quad (2.3.10)$$

$$\eta_E = \frac{E''}{E'} \quad (2.3.11)$$

and  $\eta_M = \frac{M''}{M'} \quad . \quad (2.3.12)$

Equations (2.2.4) and (2.2.5) in their complex representation become:

$$E^* = \frac{9K^*G^*}{3K^* + G^*} = \frac{9(K' + jK'')(G' + jG'')}{3(K' + jK'') + (G' + jG'')} \quad (2.3.13)$$

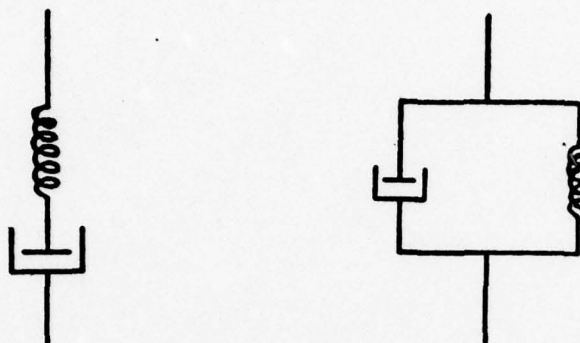
and

$$\rho^* = \frac{E^*}{2G^*} - 1 = \frac{(E' + jE'')}{2(G' + jG'')} - 1 \quad . \quad (2.3.14)$$

## 2.4 Mechanical Analogies of Viscoelastic Linear Behavior

A general mechanical representation of a viscoelastic material linear behavior can be made with a system of springs and dashpots, in series or in parallel or a combination of both.

The most simple representations are the Maxwell and Voigt<sup>2,6</sup> elements as illustrated in Figure 2.4.1:



a) Maxwell Representation      b) Voigt Representation

Figure 2.4.1. Maxwell and Voigt Simple Models of Linear Viscoelasticity.

With these model elements and extensions of them, it is possible to represent the small deformation behavior for most viscoelastic materials.<sup>6</sup>

## 2.5 Wave Propagation in Long Rods; Young's Modulus and Loss Factor

The propagation of a pressure wave in a long thin rod is represented by the following equation:

$$P = P_0 e^{-jkx} e^{-\alpha x} e^{j\omega t}, \quad (2.5.1)$$

where

$P$  = pressure at a point "x" along the rod,

$P_0 e^{j\omega t}$  = sinusoidally varying wave applied at one of the ends of the rod,

$k$  = wave number, equal to  $\omega/c$  ( $\omega$  is the frequency in radians, and  $c$  is the wave velocity),

and  $\alpha$  = attenuation constant of the material.

Equation (2.5.1) can be rewritten as:

$$P_1 = P_2 e^{-\alpha \Delta x}, \quad (2.5.2)$$

which can be solved for  $\alpha$  where:

$$\alpha = \frac{1}{\Delta x} \ln \frac{P_1}{P_2} \quad (\text{Nepers/cm}) \quad , \quad (2.5.3)$$

where  $P_1$  is the pressure wave at any point  $x_1$  along the rod and  $P_2$  is the pressure wave at a point,  $x_2 = x_1 + \Delta x$ .

Bobber<sup>7</sup> explains clearly the equations for the longitudinal wave propagation in a rod together with its related components. Using an electrical analogy with an acoustic transmission line, he finds that the loss factor  $\eta$  of a viscoelastic material is given by:

$$\eta = \frac{2r}{(1 - r^2)} \quad , \quad (2.5.4)$$

where

$$r = \frac{\alpha \lambda}{2\pi} \quad , \quad (2.5.5)$$

$r$  being the loss parameter in Nepers,  $\lambda$  is the wavelength of the vibration, and  $\alpha$  is the attenuation constant.

Nolle<sup>8</sup> defines the storage Young's modulus as:

$$E' = \rho c^2 \frac{(1 - r^2)}{(1 + r^2)^2} \quad , \quad (2.5.6)$$

where  $\rho$  is the density of the material,  $c$  is the velocity of the wave, and  $r$  is the loss parameter. From this equation and Equations (2.3.1) and (2.3.11), the Young's loss modulus is given by:

$$E'' = \eta E' = \rho c^2 \frac{(1 - r^2)}{(1 + r^2)^2} \eta \quad . \quad (2.5.7)$$

The classical relation for Young's modulus states that:

$$E = \rho c^2 \quad (2.5.8)$$

which defines only purely elastic propagation.



## 2.6 Frequency and Temperature Dependence

It was mentioned before that viscoelastic materials show a great dependence on frequency and temperature. This dual dependence is also inter-related. In fact, when the temperature of a viscoelastic material is increased, its internal molecular arrangement changes and becomes more mobile, hence, more elastic, whereas when the temperature is reduced, the molecular mobility is reduced, hence, the material becomes stiffer and presents glass-like properties.

On the other hand, if the temperature of an elastomer is kept constant and the stress frequency is increased or decreased, a similar but inverse phenomenon occurs. At low frequencies, the period of stress is sufficiently long for the molecules to coil and uncoil; therefore, the material presents rubber-like properties. At high frequencies, the period of stress is very small and the material presents glass-like characteristics.

Tobolsky<sup>9</sup> conducted studies of stress relaxation phenomena on polymethyl-methacrylate of two different molecular weights under constant stress and, from the data obtained, drew curves of Young's modulus versus time and described four regions in the behavior of a viscoelastic material:

- (a) A low temperature, glassy region, where the Young's modulus is almost constant. The time dependence of the modulus is quite independent of the molecular weight, but dependent on the annealing rate of the sample.
- (b) A transition region where the Young's modulus changes very rapidly with time and temperature, ranging from  $10^{10}$  to  $10^7$  dynes/cm<sup>2</sup>.

- (c) A quasi-static rubbery plateau region, where the modulus remains more or less the same, at about  $10^7$  dynes/cm<sup>2</sup>.
- (d) A flow region where the values of the modulus drops very quickly to almost zero.

Figure 2.6.1 gives a graphic idea of these regions.

In the description of a viscoelastic material, three rather than four regions are sufficient when considering the general moduli, especially if the loss factor behavior is taken into account. These three regions are the rubbery region, the relaxation region, and the glassy region, as shown in Figure 2.6.2. In this consideration, the storage modulus at high temperatures or low frequencies is almost constant, but as the temperature is reduced or the frequency increased, the modulus shows a rapid increase until a point is reached where the modulus keeps nearly constant. The region of rapid increment is the relaxation region, and the other two are the rubbery region (high temperatures or low frequencies), and the glassy region (low temperatures or high frequencies).

The loss factor follows a different pattern. In the rubbery region, this factor is almost constant, increasing just a little with increasing frequency or decreasing temperature. In the relaxation region, it increases enormously, reaching a maximum point called the transition point, and from there, it decreases until it reaches another plateau where the factor is again almost constant; then, the material is in the glassy region.

The transition point is different for different materials; for example,  $-73^{\circ}\text{C}$  for rubber, and  $100^{\circ}\text{C}$  for polystyrene.<sup>10</sup>

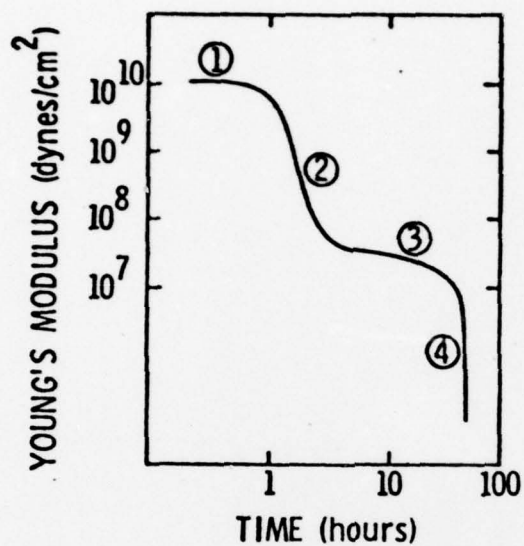


Figure 2.6.1. Tobolsky Regions of Viscoelastic Behavior Based on Creep Experiments.

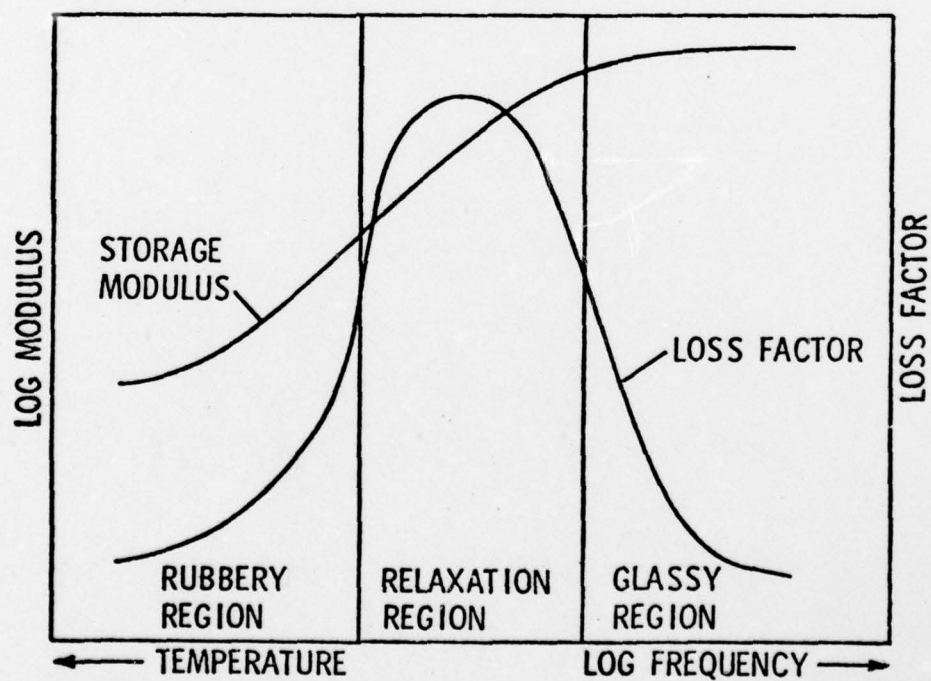


Figure 2.6.2. Behavior of Viscoelastic Moduli.

Ferry<sup>11</sup> gives a thorough description of the molecular theory of polymers. In Chapter XI, he describes the dependence of viscoelastic materials on temperature at different frequencies. He concludes, by using mechanical models, that frequency and temperature are inversely related and a procedure known as the WLF transformation is stated. This transformation requires the change of abscissa from  $\log \omega$  into  $\log \omega a_T$  where:

$$-\log a_T = \frac{C_1^0(T - T_0)}{(C_2^0 + T - T_0)} \quad (2.5.9)$$

$a_T$  is the ratio of any specific relaxation time at a certain temperature  $T$ , to its value at an arbitrary reference temperature  $T_0$ . The relaxation time is the time required for the stress in each mechanism to relax to  $1/e$  of the initial stress induced by a suddenly applied constant strain, and  $C_1^0$  and  $C_2^0$  are constants for the material.



## CHAPTER III

### EXPERIMENTAL SET-UP FOR TENSILE TEST

#### 3.1 Kuehl and Meyer Technique

Different methods exist to test the dynamic tensile characteristics of viscoelastic materials. Two approaches with slight variations are henceforth described. The first approach, after the experiments made by Kuehl and Meyer,<sup>12</sup> presented various technical difficulties. The second, after Nolle's experiment,<sup>13</sup> was the experiment from which data included in Chapter IV was obtained.

Figure 3.1.1 shows schematically the apparatus as used by Kuehl and Meyer for the determination of sound velocity and attenuation constant in elastomers. The elastomer strip hangs in a column of water from an electromechanical shaker driven by an Electrodyne-Oscillator. The shaker rested on a triangular plate with perforated corners in order to slide the plate over a three rod mount and thus, attain perpendicularity. A screw nut in each rod helped to tighten and fix the position at each corner. By this means, the elastomer could be moved in and out of the water. The other end of this elastomer was connected to a thread which passed through a hook in the bottom of the water column and was connected to the external part through a small hole in the lid of the tube. This way the string could be pulled to provide some tension on the elastomer.

The sound that the elastomer radiates into the water is measured by a very sensitive hydrophone which enters the water tube

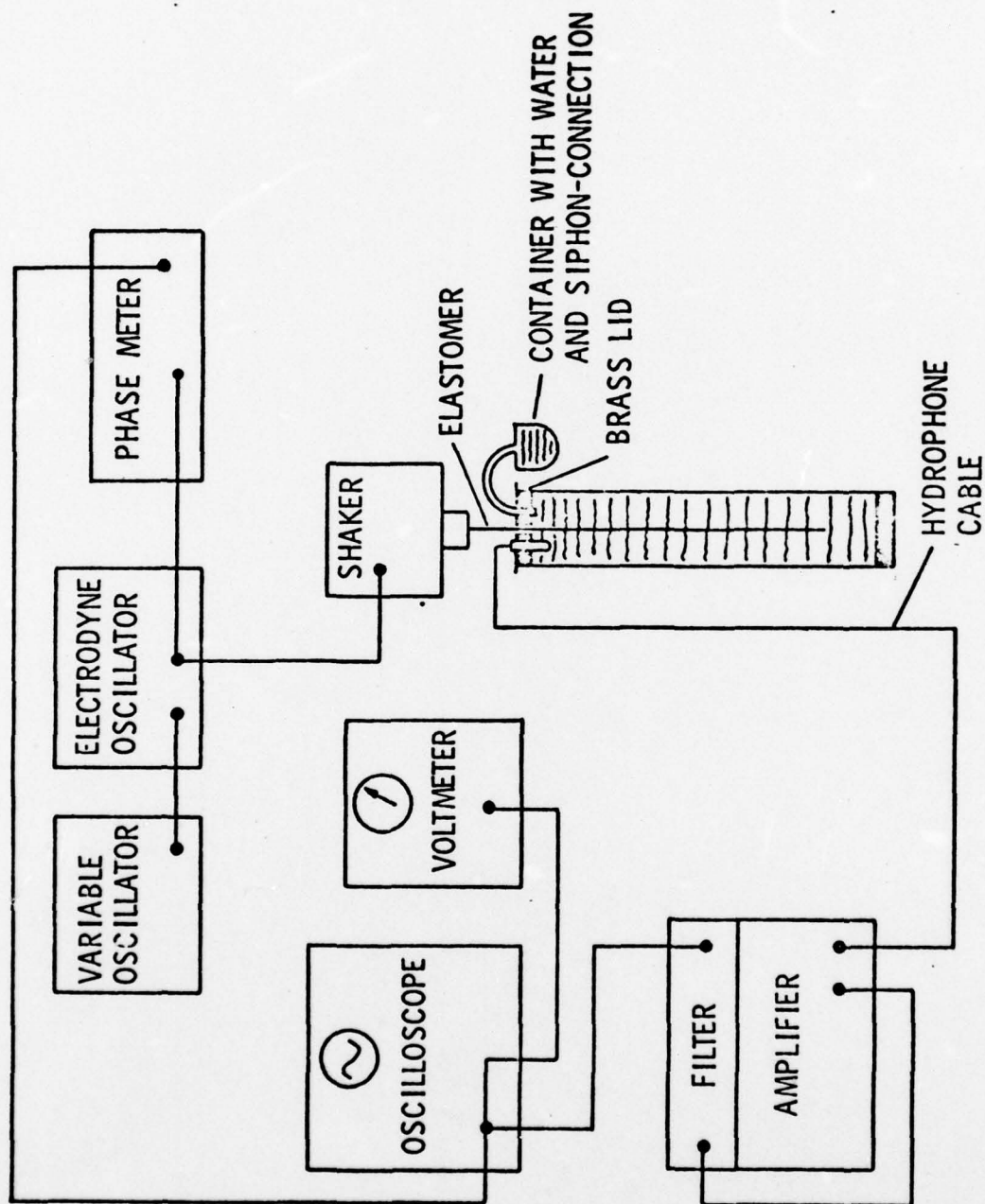


Figure 3.1.1. Apparatus to Test Longitudinal Wave Propagation; Technique of Kuehl and Meyer.

through a hole in the lid. The purpose of this was to provide the water surface with a hard surface having a mass large enough such that its mass impedance is equal or larger than the wave impedance of the fluid. In this way, the sound pressure at the top of the tube becomes an antinode and hence has a maximum pressure level. From that point on, the pressure wave pattern in the tube is that of a standing wave. In order for the water level to remain constant when moving the elastomer in and out of the water, a siphon tube was connected through the lid into the water with its other end connected to a small water container. The hydrophone was connected to an amplifier and to a band pass filter before the wave signal was registered by a voltmeter. An oscilloscope helped to observe the signal level. A phase meter was connected to the signal being registered by the voltmeter, and to the electrodyne-oscillator providing the original sinusoidal input signal. The general circuit can be observed in Figure 3.1.1. Since the hydrophone cable was extremely sensitive, precautions were taken to isolate and ground it.

The transmission of vibrations between the shaker and the triangular plate was improved by means of rubbery mounts separating them from direct metal to metal contact.

It was also recommended by Kuehl and Meyer to isolate the entire tube against air sound with a thick mineral wool shell; this precaution was not taken in this experiment. The hydrophone kept picking up a large amount of external noise of both acoustic and electric origin and, of the measurements made of the sound propagation in some materials, almost no reliable information could be obtained; therefore, a different experimental setting was made, this time using a light record player stylus to pick-up the vibrations on the elastomer.

### 3.2 Nolle's Technique

Kuehl and Meyer, prior to their experiment, rejected the measuring of advancing waves with a pick-up stylus on a thin elastomer because they could not get data beyond 5 kHz. Nolle,<sup>13</sup> however, presented some results of up to 26 kHz. Therefore, by using some of the equipment already described in the last section, a new experiment was set up to expand on Nolle's method.

The shaker was still suspended by resting on the triangular plate and the three rods. The elastomer connected to the shaker was to remain fixed for the pick-up to scan its surface, so a position for the shaker was chosen and the screws were set in a definite position during the entire experiment. The pick-up consisted of a stereo pick-up stylus and it was mounted on a triaxial vernier screw mechanism which allowed accurate displacement in three dimensions. In this fashion, the stylus touched the elastomer with the required tracking force of 1-1/2 to 2 grams along the center of the face of the elastomer on which measurements were made. A simple diagram of the vernier mechanism and shaker with elastomer is shown in Figure 3.2.1.

Samples of viscoelastic materials of 1/16 x 1/16 inch cross section and 12 inches long were attached to the shaker which was connected to an electrodyne oscillator and this to a variable oscillator capable of operating up to 100 kHz. This extreme frequency range was not necessary, however, as the cartridge was incapable of operating above 45 kHz. The other end of the sample was connected to a piece of thread whose purpose was to put a small tension on the sample and maintain alignment.



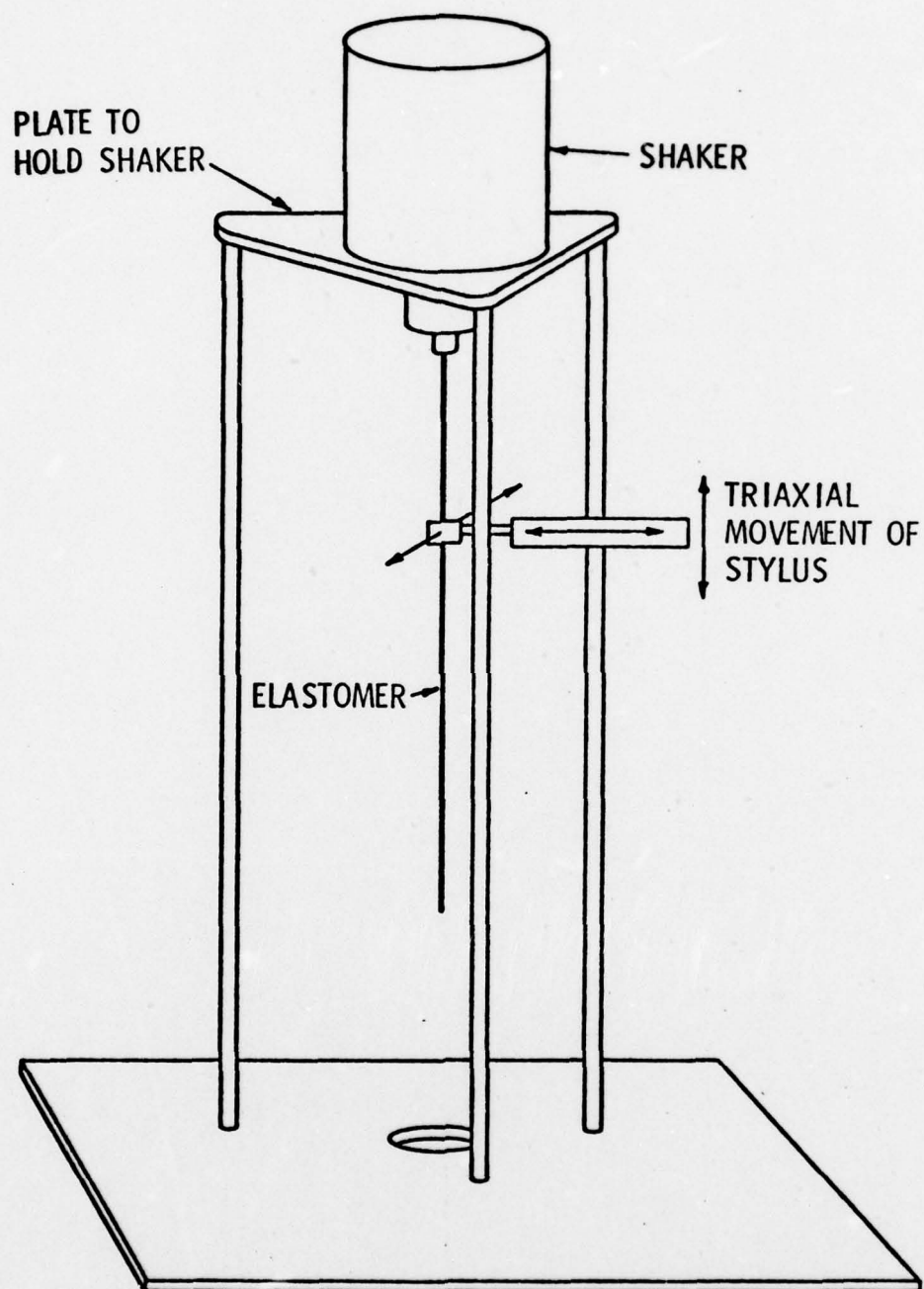


Figure 3.2.1. System of Triaxial Rulers.

When the elastomer is under a sinusoidally vibrating stress, as is the case in this experiment, there is a compressional wave travelling through it. Transverse waves are excited at the same time. Both signals were thought to be detectable by means of the two stereo components of the pick-up stylus used. This process is explained with clarity in Section 3.4.

After the signals were detected, they were amplified, filtered from noise and measured by the voltmeter. The signal measured is the particle velocity of the travelling wave. A phase meter was connected to the output of the oscillator and to the output of the filtered signal. A double beam oscilloscope helped to easily follow the changes of phase of the signals. A frequency meter connected to the negative terminal of the oscillator helped to select the exact frequency of operation. Inasmuch as force is in phase with driver current, a resistor was placed in series with the driver coil and the drop across this resistor was monitored for the phase. The general circuit is shown in Figure 3.2.2.

### 3.3 Characteristics of the Pick-up System

The pick-up system consisted of an Audio-Technica dual magnet phonograph cartridge, Model AT-12-E, having the following characteristics:

Frequency Response	15 - 45,000 Hz
Output at 5 cm/sec	3.5 mV
Channel Separation at 1 kHz	22 dB
Channel Balance	2 dB
Tracking Force	1-1/2 - 2 grams
Vertical Tracking Angle	20°

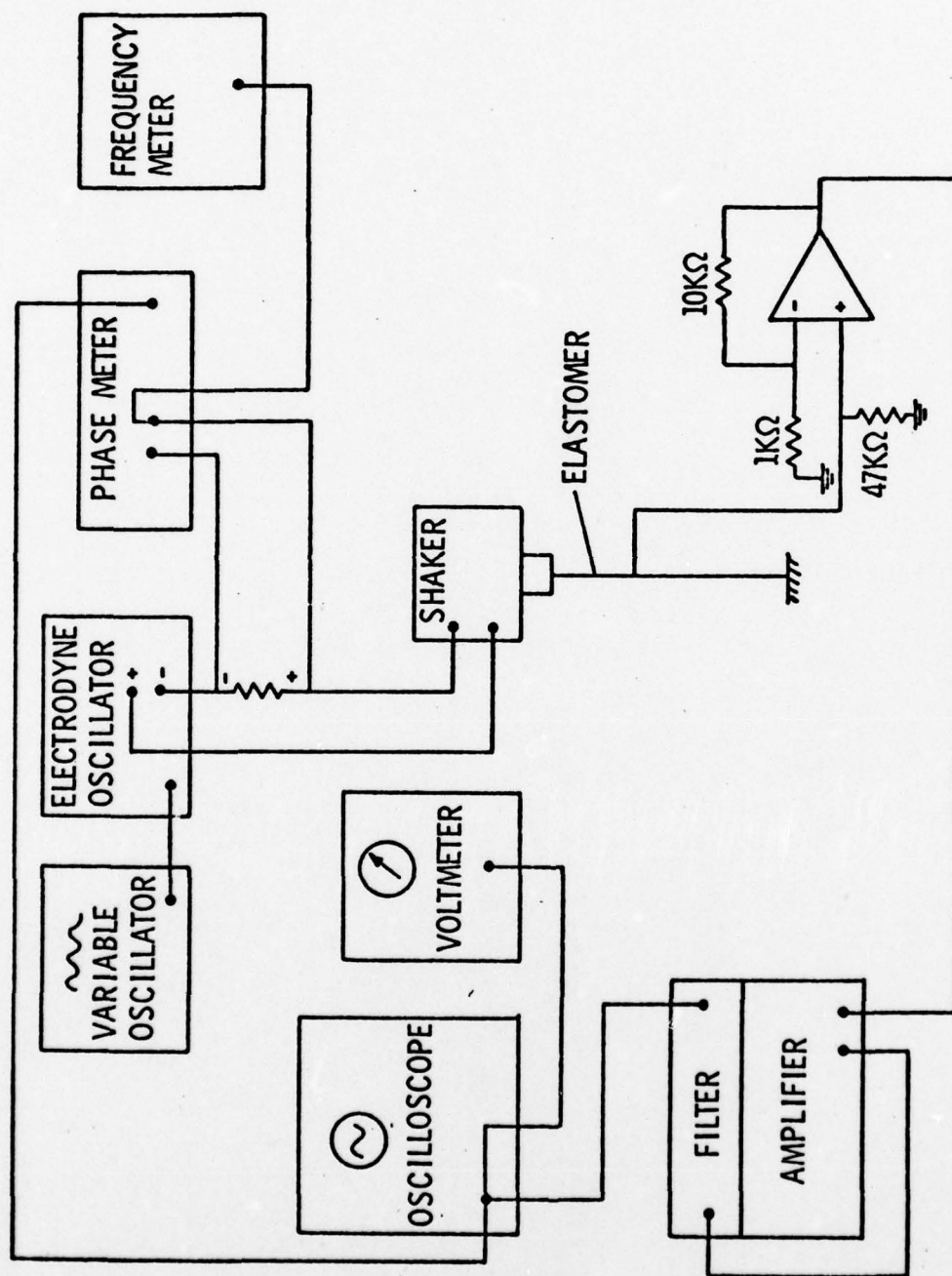


Figure 3.2.2. Electronic Box-Diagram for Measurement of Wave Propagation on an Elastomer; Technique of Nolle.

Load Impedance	47 k $\Omega$
Cartridge Inductance	670 mH
DC resistance	1300 $\Omega$

The frequency response gives the limits of frequency testing in this experiment. The minimum frequency in which measurements were taken was 500 Hz and the maximum 25,000 Hz. The cartridge arm consisted of a tube similar to those used in a record player, with a support for the cartridge having a 20° slope to compensate for the vertical tracking angle. Care to provide a force of 2 grams through all the measurements made was taken. The cartridge uses two permanent magnets mounted at an angle of 45°. These, when working on a record, are perpendicular to the two sides of the groove. With its pole pieces and electrical coils, each magnet becomes an electrical generator reproducing mainly the signal from one side of the record groove, with a maximum of 22 dB cross-talk from the other channel. This was a very important factor in the measurements of both the extensional and the transverse wave signal. The cartridge translates into an electrical signal the particle velocity of the wave at a rate of 3.5 mV per 5 cm/sec. Each stereo channel has an output and ground connections which can be connected for monaural operation by joining the left and right pick-up coils together in parallel. With this monaural connection, the vertical output of the cartridge is cancelled so that the longitudinal excitation is the only one obtained.

In order to reduce the output impedance of the cartridge, an operational amplifier was used. It had a double purpose, one to reduce the load impedance from 47 k $\Omega$  to just a few ohms, and to act as a 10 dB amplifier to reduce electrical noise interferences.



### 3.4 Relation Between Stereo Signal and the Longitudinal and Transverse Waves

A stereo record has information recorded on both sides of a  $90^\circ$  V-shaped groove; therefore, the information on one side is largely independent of the information on the other side of the groove. Figure 3.4.1 shows a schematic view of the groove undulations in a stereophonic disc phonograph record. A is the unmodulated groove; B is the modulation in the right channel; C is the modulation in the left channel; D is the lateral modulation formed by the combination of right and left modulations in phase; E is the vertical modulation or combination of right and left modulations out of phase, and F is the combination of equal vertical and lateral amplitudes. Heavy lines in the figure indicate zero amplitude or unmodulated groove. Dashed lines indicate maximum limit of groove undulation. Arrows indicate direction of motion of the reproducing stylus.<sup>14</sup>

In a sound reproducing system, the stylus follows the undulation in the groove of a rotating record and transfers the vibration of the stylus to the pick-up transducers. In the case of this experiment, the stylus picks up the vibration from the travelling wave in the elastomer and transfers it to the transducers in the cartridge. Figures 3.4.2 and 3.4.3 show the direction of the particle motion of both the longitudinal or dilatational wave and the transverse wave, respectively.<sup>4</sup>

Figure 3.4.4 shows graphically the two signals along the elastomer and the stylus on it. Figure 3.4.5 shows how a record player acts over the same stylus. By these illustrations, it is seen that the signals in the elastomer are detected as vectorial components

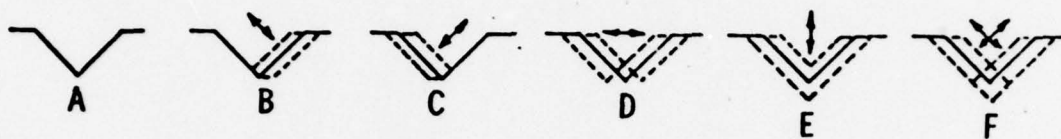


Figure 3.4.1. Schematic View of Groove Undulations in a Stereophonic Disc Phonograph Record.

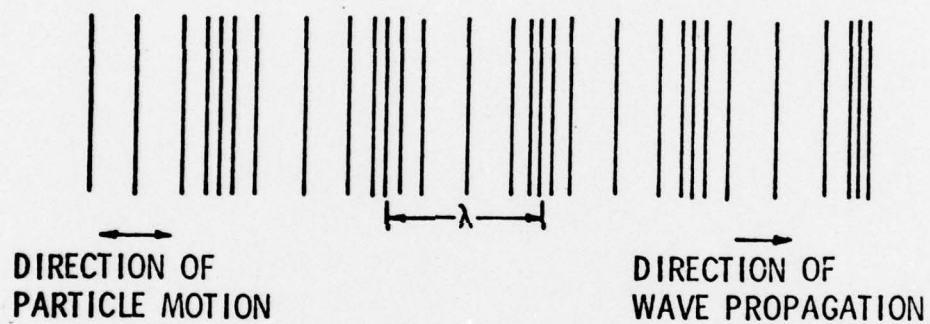


Figure 3.4.2. Particle Motion for Longitudinal Wave.

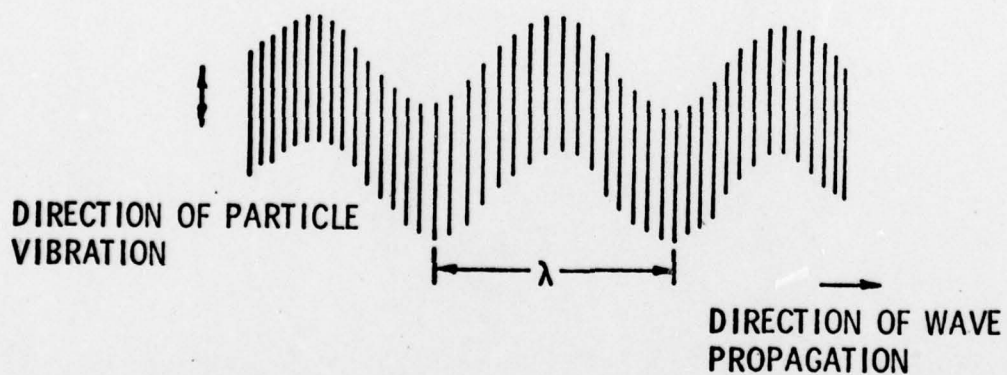


Figure 3.4.3. Particle Motion for Transverse Waves.

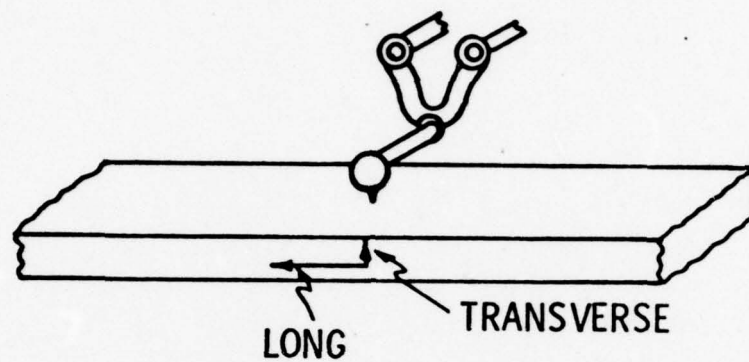


Figure 3.4.4. Longitudinal and Transverse Signals on an Elastomer.

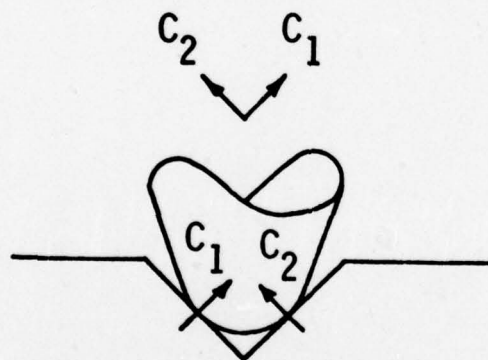


Figure 3.4.5. Stylus on a Record Player Groove.

at  $45^\circ$ ; i.e., the longitudinal travelling wave is given vectorally by  $C_2 - C_1$  and the transverse travelling wave by  $C_2 + C_1$  as shown in Figure 3.4.6.

According to the process explained, both the left and right signals from the pick-up stereo were expected to be obtained. There were, however, many difficulties in doing so; a perfect alignment between the elastomer and stylus was very important in the measurements of the transverse wave and this was difficult to achieve. Two other problems were interference between channels and flexural waves. These problems led to connecting the two stereo channels into a monaural pick-up, hence, recording only the longitudinal travelling wave. In Section 3.6, some of these problems are explained.

### 3.5 Materials Tested

Samples of eight viscoelastic materials were prepared by molding them in a metal mold whose cross section was  $1/16 \times 1/16$  inch and 12 inches long. Figure 3.5.1 shows the shape of the samples and their base which serves to attach the elastomer to the shaker by means of a screw.

The different elastomers tested were:

- (a) Castomold Polyester
- (b) EN-6 Polyurethane
- (c) Hypalon H-862 synthetic rubber
- (d) PRC-1564 polyurethane
- (e) Butyl B-252 synthetic rubber
- (f) Natural Rubber 33001
- (g) Neoprene 33003, and
- (h) PRC-1524 polyurethane



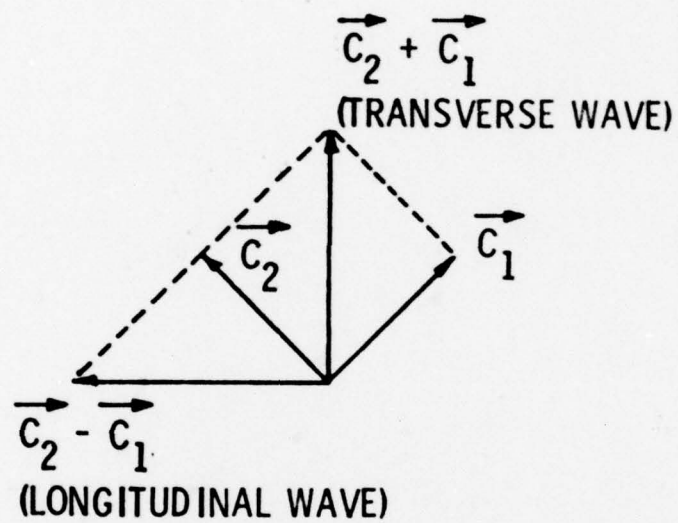


Figure 3.4.6. Vectorial Components of Longitudinal and Transverse Wave.

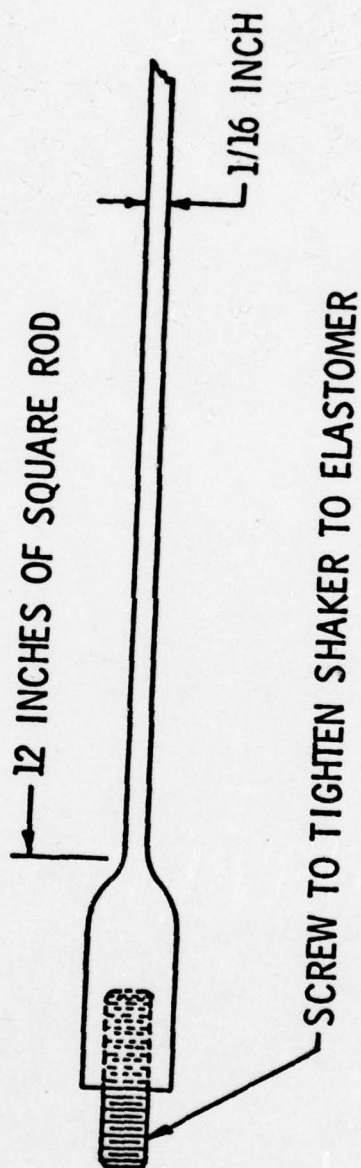


Figure 3.5.1. Elastomer Sample

These particular materials were chosen as being representative of those used in sonar applications.

### 3.6 Experimental Problems

Flexural Waves. When data were taken, it was noticed that the transverse wave signals displayed two different wavelengths, which meant that an external signal was interfering with the measurements. Figure 3.6.1 shows graphically these different wavelengths for a single frequency of excitation. This example corresponds to the sample of Polyurethane EN-6 at a frequency of 12,040 Hz.

The mathematical expression for the propagation speed of flexural waves is related to that for compressional waves in a rectangular material by:<sup>15</sup>

$$\frac{C_f^2}{C_c} = \frac{h\omega}{\sqrt{12}}, \quad (3.6.1)$$

where  $h$  is the width of the sample (1/16 inch),  $\omega$  is the frequency in radians/sec ( $2\pi f$ , where  $f = 12,040$  Hz) and  $C_f$  and  $C_c$  are defined by the following equations:

$$C_c = \sqrt{E/\rho} \quad (3.6.2)$$

and

$$C_f = [(h^2 \omega^2 C_c^2)/12]^{1/4} \quad (3.6.3)$$

Substituting values for  $C_f$  and  $C_c$ , where  $C_f = \lambda_1 f$  and  $C_c = \lambda_2 f$ , with  $\lambda_1 = 0.98$  cm and  $\lambda_2 = 3.03$  cm as obtained from Figure 4.2.1,  $C_f^2/C_c = 38.2$  m/sec. Substituting values in Equation (3.6.1),  $h\omega/\sqrt{12} = 34.7$  m/sec.

These values are very close to each other and this fact led to the conclusion that both flexural and longitudinal waves were propagating along the rod.

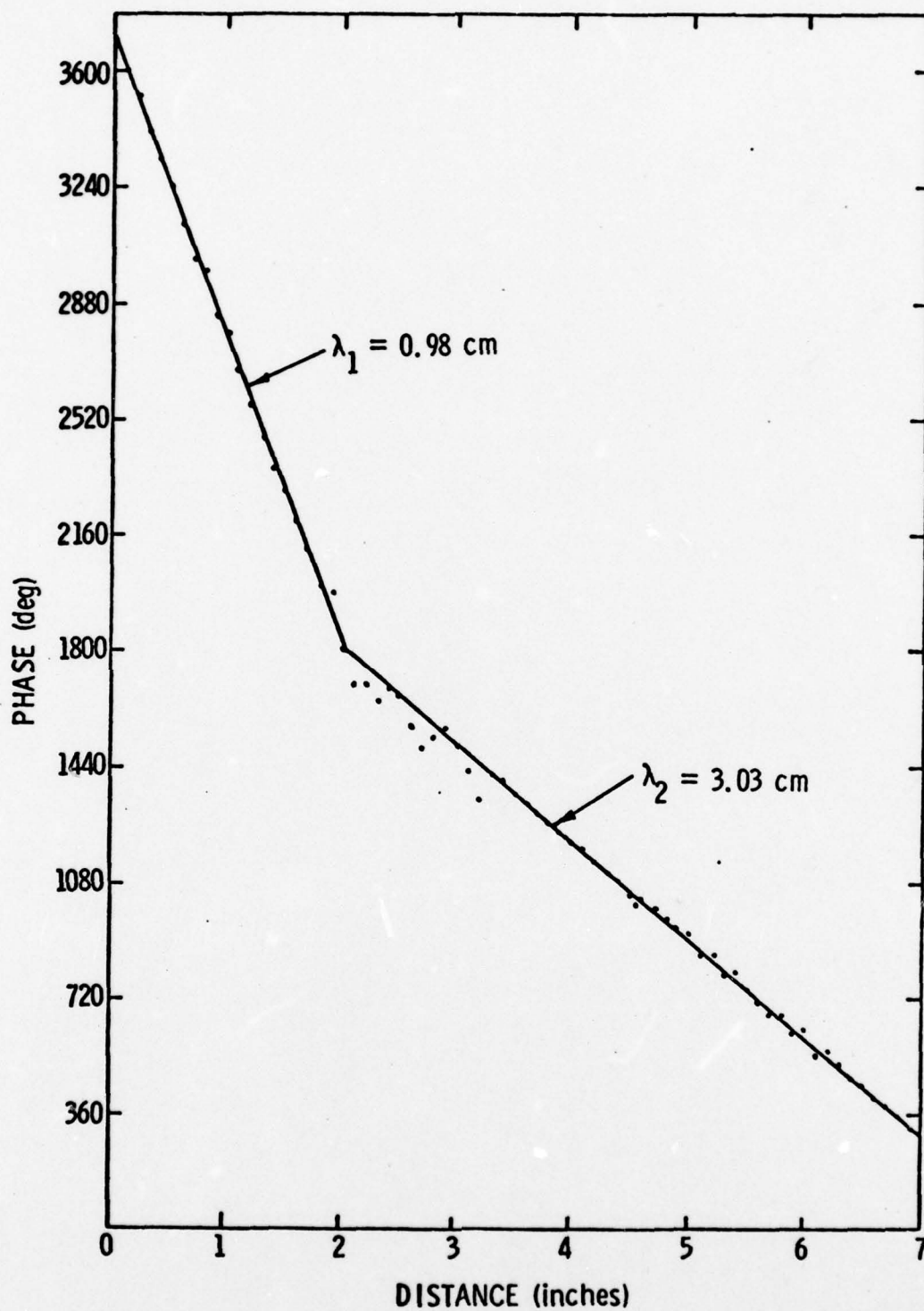


Figure 3.6.1. Measurement of Transverse Waves with Flexural Waves as a Disturbance.



The flexural wave velocity increases with increasing frequency with the result that, while at low frequencies, the flexural waves are attenuated rapidly, at sufficient high frequencies, flexural waves are observed throughout the whole length of the elastomer.<sup>8</sup>

This flexural wave effect is noticeable at lower frequencies for materials having low dynamic modulus.

In an attempt to avoid the flexural waves which could be caused by the misalignment of the elastomer and shaker, a solid string and a weight were connected between them as seen in Figure 3.6.2. By this means the longitudinal waves should be the only ones travelling down the piece of wire avoiding the transmission of flexural waves. This idea was not effective as the mass acted as a low pass filter and attenuated both waves.

Noise problems. Two noise problems were affecting the experiment, electrical and vibrational ones. The electrical noise was improved when some of the external connections were grounded; among them, the wires from the pick-up cartridge, the connection between the oscillator and shaker, and the connection between the oscillator and the phase meter. Vibrational noises were prevented by rubber mounts between metal surfaces. For all recorded data, a signal-to-noise ratio greater than 10 dB was required.

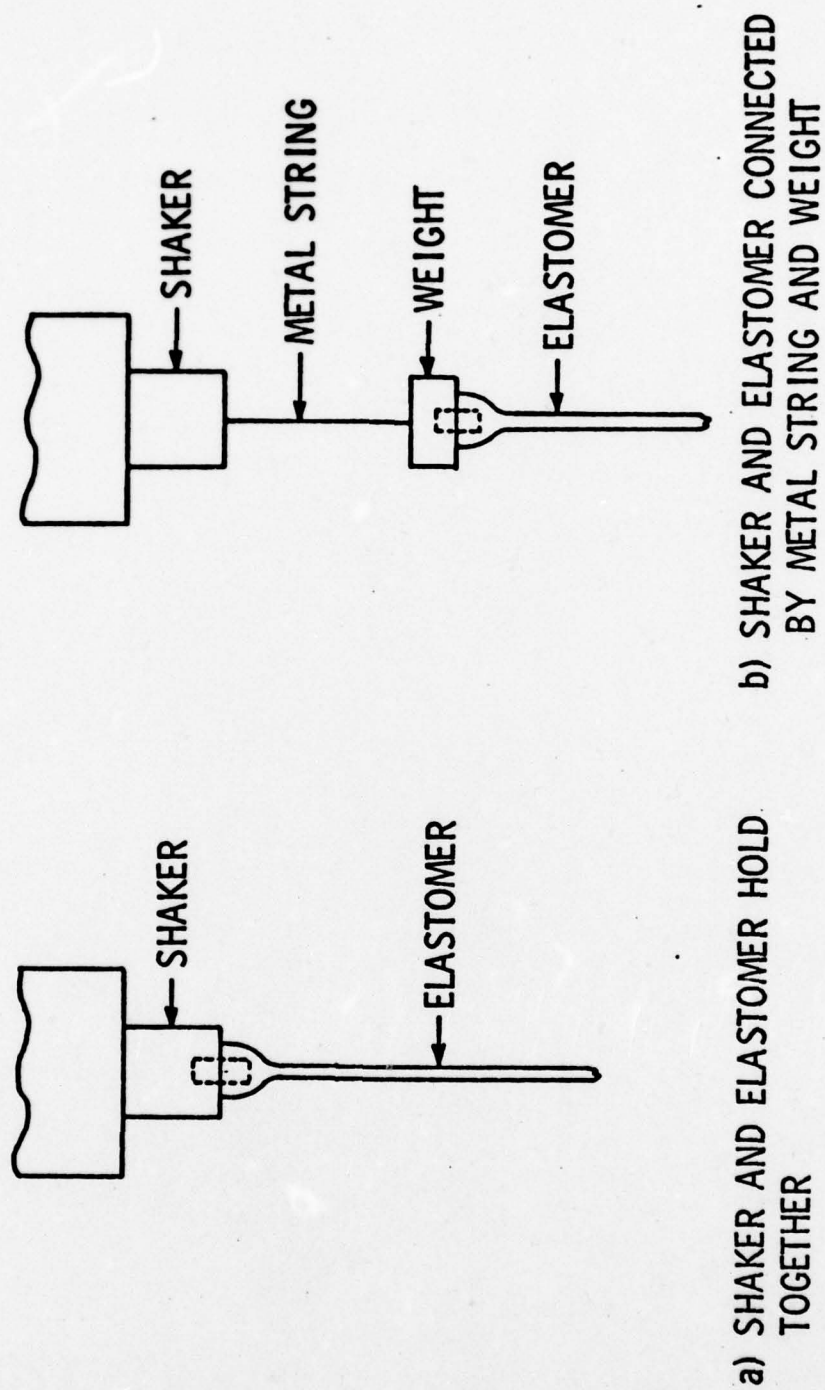


Figure 3.6.2. Connections Between Shaker and Elastomer.

## CHAPTER IV

### EXPERIMENTAL RESULTS

#### 4.1 Reduction and Interpretation of Data

The final measurements in this experiment involved reading of the longitudinal particle velocity signals together with their phase difference. For each frequency of vibration, recordings of distance along the elastomer to every measuring point, voltage and phase difference were taken. These data were plotted in two different curves, one of phase difference versus distance, and another of longitudinal signal amplitude versus distance.

All measurements were taken at temperatures of between 28 and 29 degrees Centigrade.

When plotting phase versus distance, curves similar to that of Figure 4.1.1 are obtained. Values of the wavelength for each frequency are obtained as indicated on the figure.

The graph of voltage versus distance is an exponentially decaying curve, so that on a semilog paper, typical straight lines like that of Figure 4.1.2 can be drawn. The slope represents the attenuation of the sound wave as it propagates along the rod. Using this plot, values for the attenuation constants for the various materials were obtained utilizing Equation (2.5.3).

These two plots were drawn at several frequencies for each one of the materials tested. The lower frequency limit was established when the length of the sample was one-half wavelength of the wave transmitted or when the attenuation was so small that some reflections

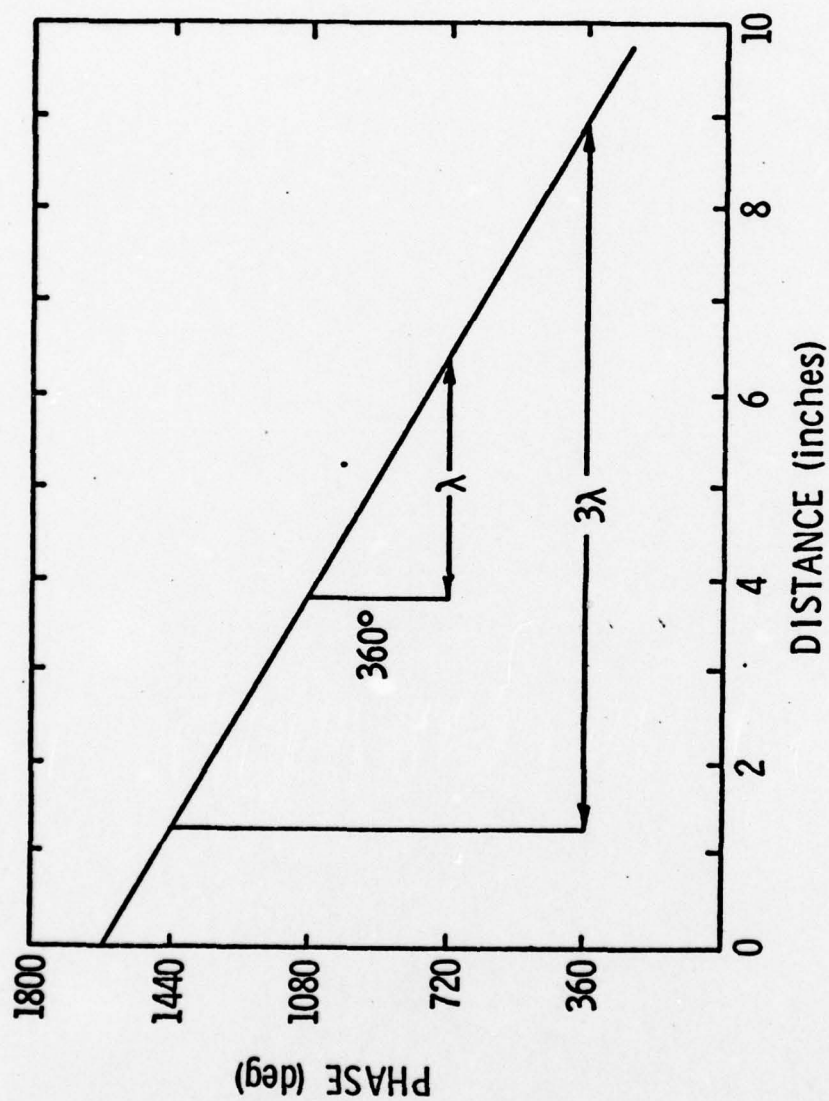


Figure 4.1.1.1. Typical Phase Difference as a Function of Distance.



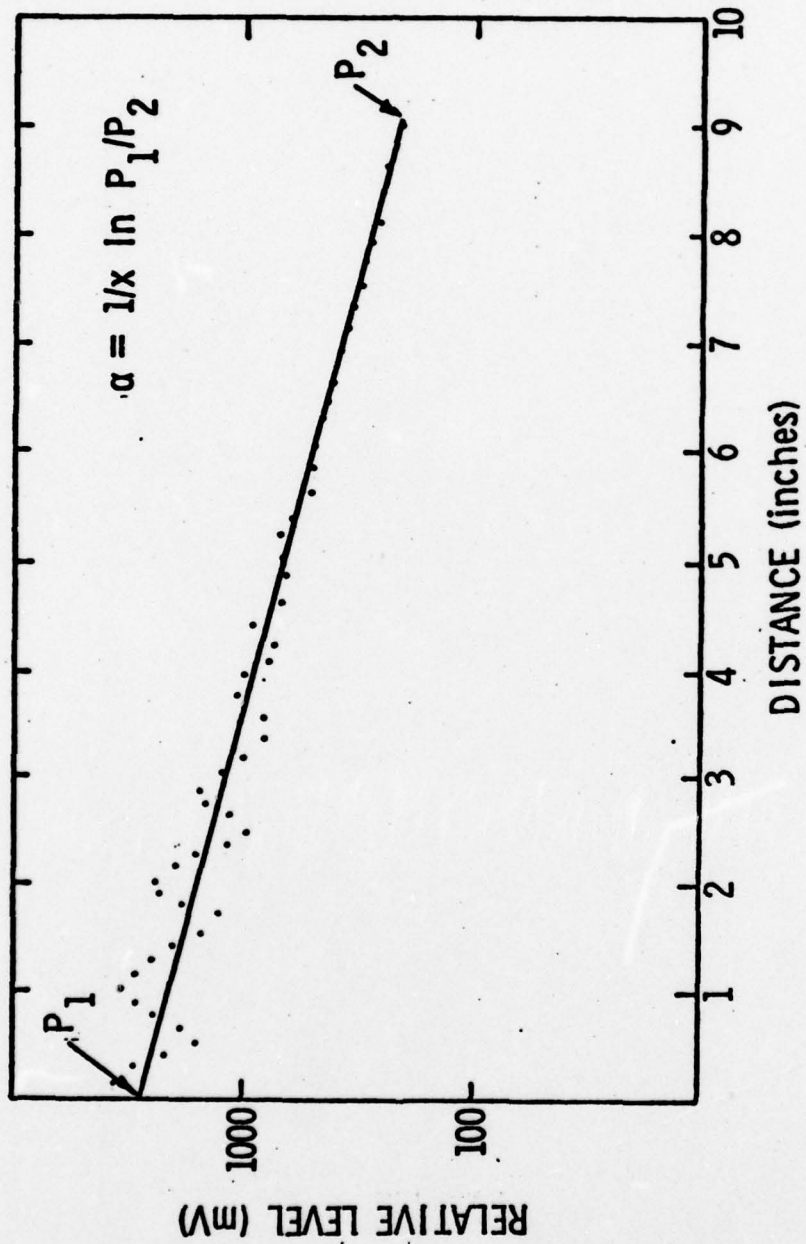


Figure 4.1.2. Typical Wave Pressure as a Function of Distance.

occurred. The higher frequencies measured were limited by the attenuation constant which increases with increasing frequency and by the noise of the system.

With the results for attenuation constant obtained, new graphs of attenuation constant versus frequency were drawn. The values were smoothed graphically before other physical properties were calculated. Figure 4.1.3 shows a typical attenuation graph.

With these new values of the attenuation constant  $\alpha$ , values for the loss parameter  $r$ , the loss factor  $\eta$ , and values for the static  $E$ , and dynamic  $E'$ ,  $E''$ , Young's modulus were calculated by using Equations (2.5.4) through (2.5.9).

#### 4.2 Young's Modulus and Loss Factor Results

The experiments and observations made from the different samples are summarized in the following tables and graphs. Some of these materials have various frequency limits depending upon the attenuation constant, noise, reflections and wavelength in the particular sample.

Two figures are shown for each material, one corresponding to the attenuation constant and the other including loss modulus, storage modulus and loss factors of the materials.

The density of each material is specified on each figure.

Figures 4.2.1 to 4.2.16 include two figures for each of the following materials, respectively:

- (a) Castomold Polyester
- (b) EN-6 Polyurethane
- (c) Hypalon H-862
- (d) PRC-1564

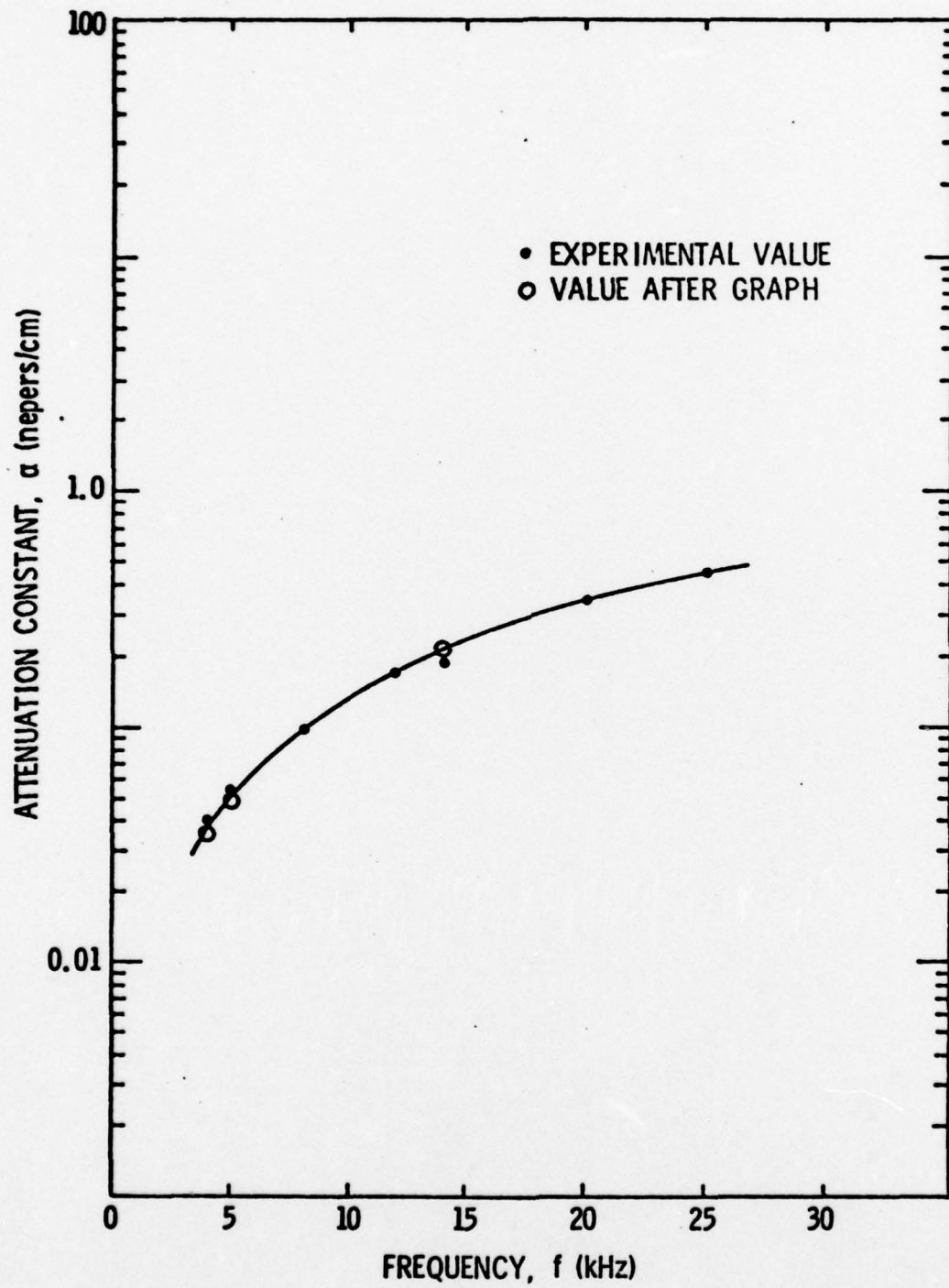


Figure 4.1.3. Typical Attenuation Constant Versus Frequency.

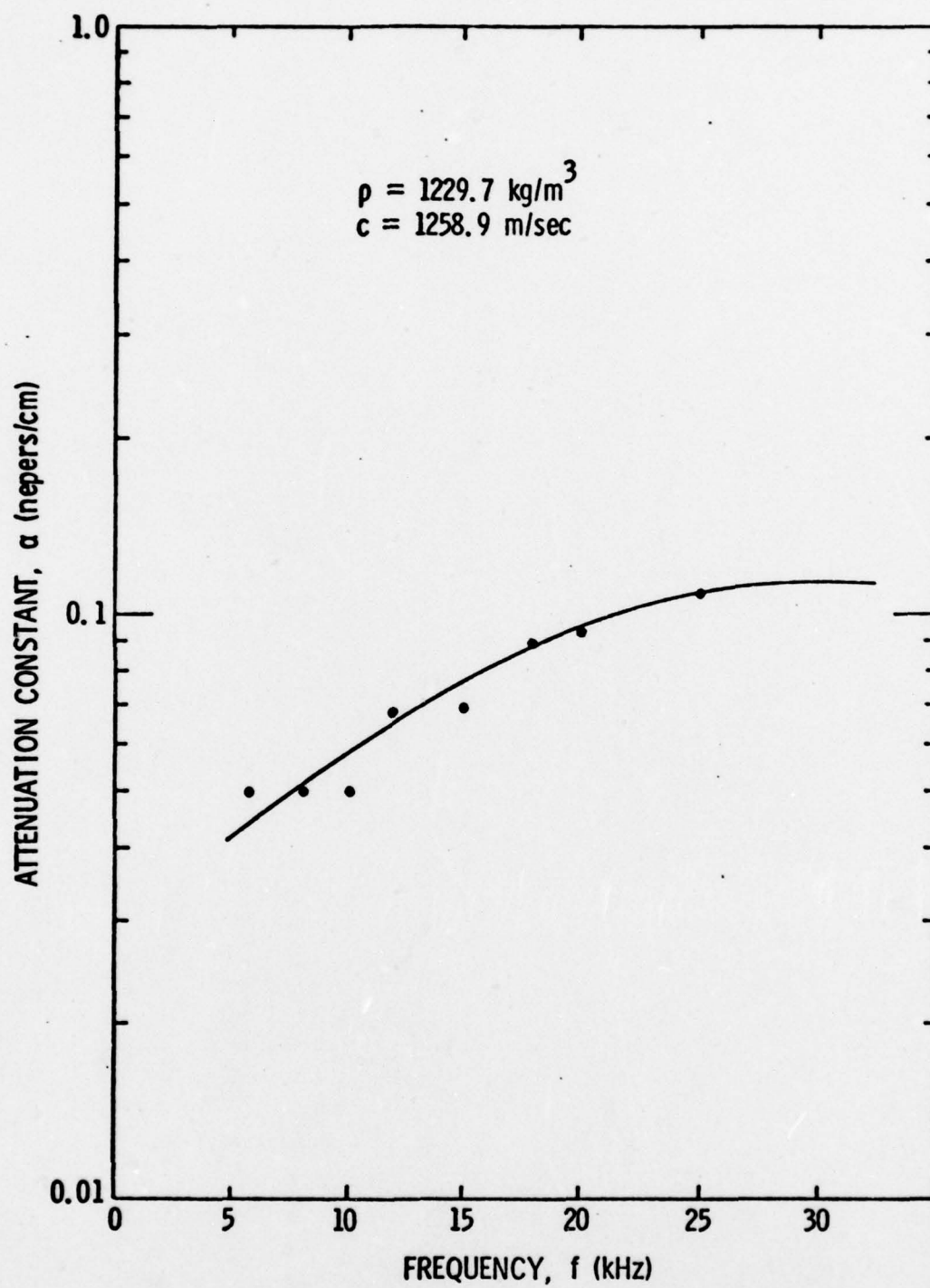


Figure 4.2.1. Attenuation Constant for Castomold Polyester.



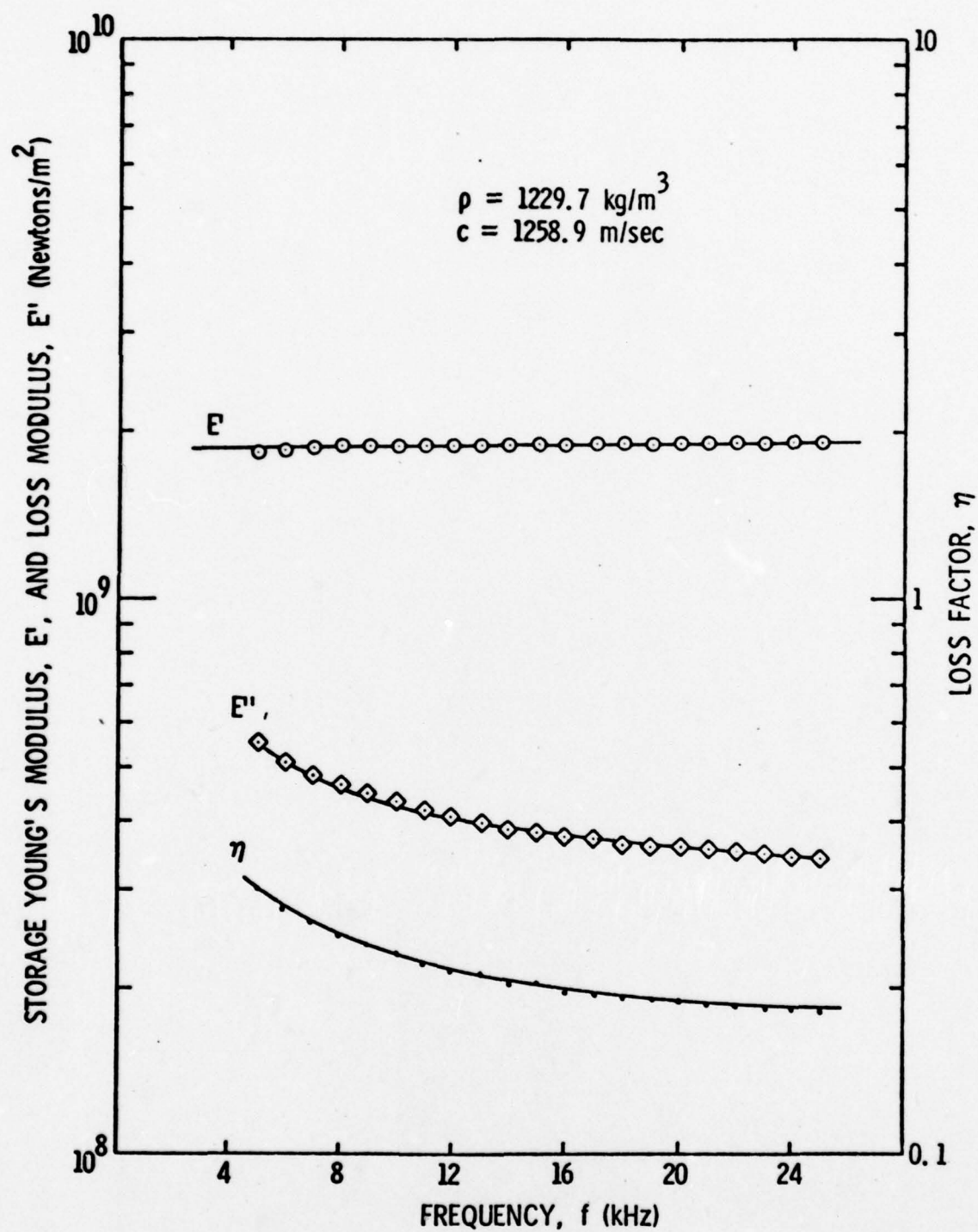


Figure 4.2.2. Storage and Loss Young's Modulus and Loss Factor for Castomold Polyester.

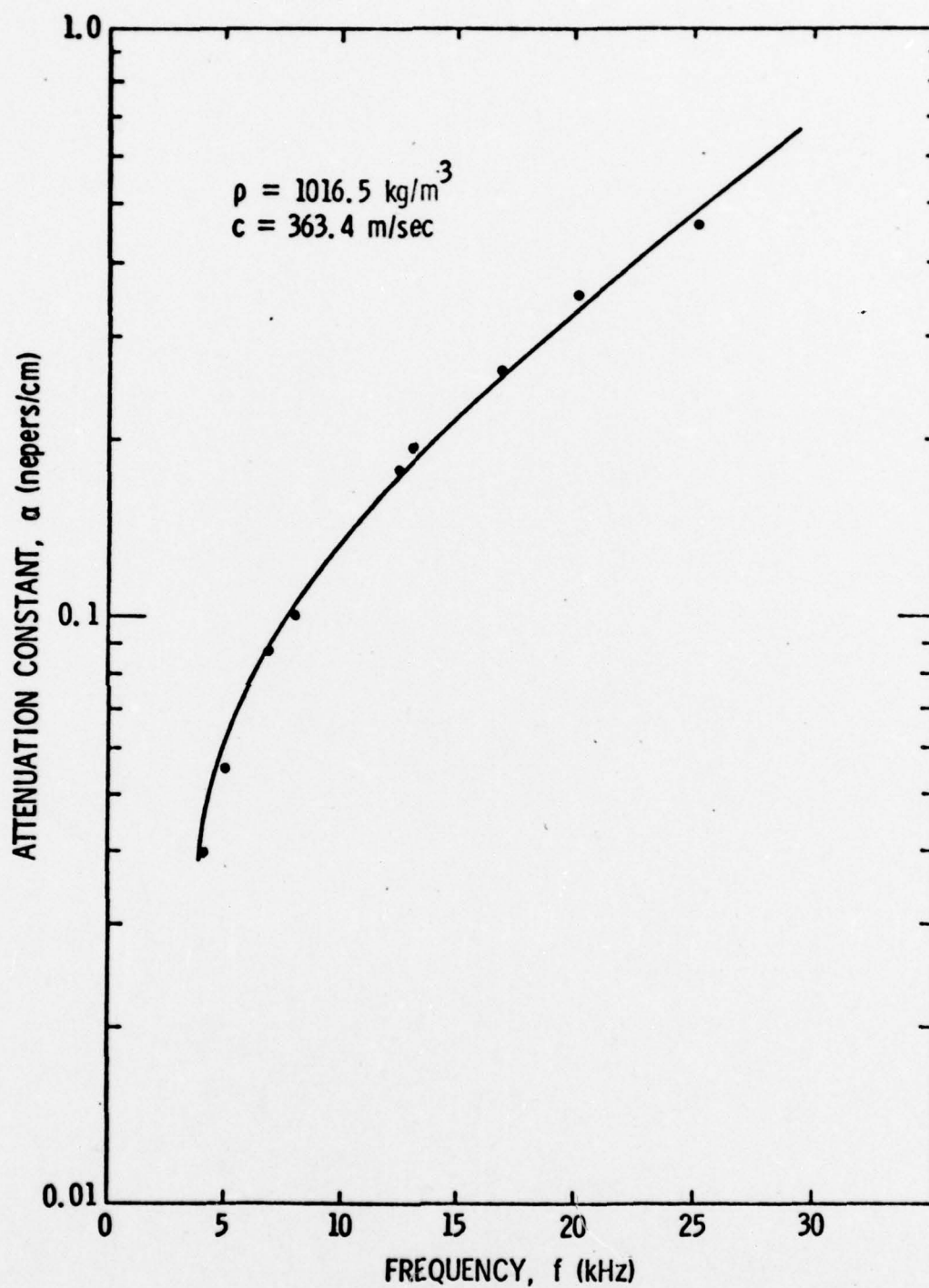


Figure 4.2.3. Attenuation Constant for EN-6 Polyurethane.

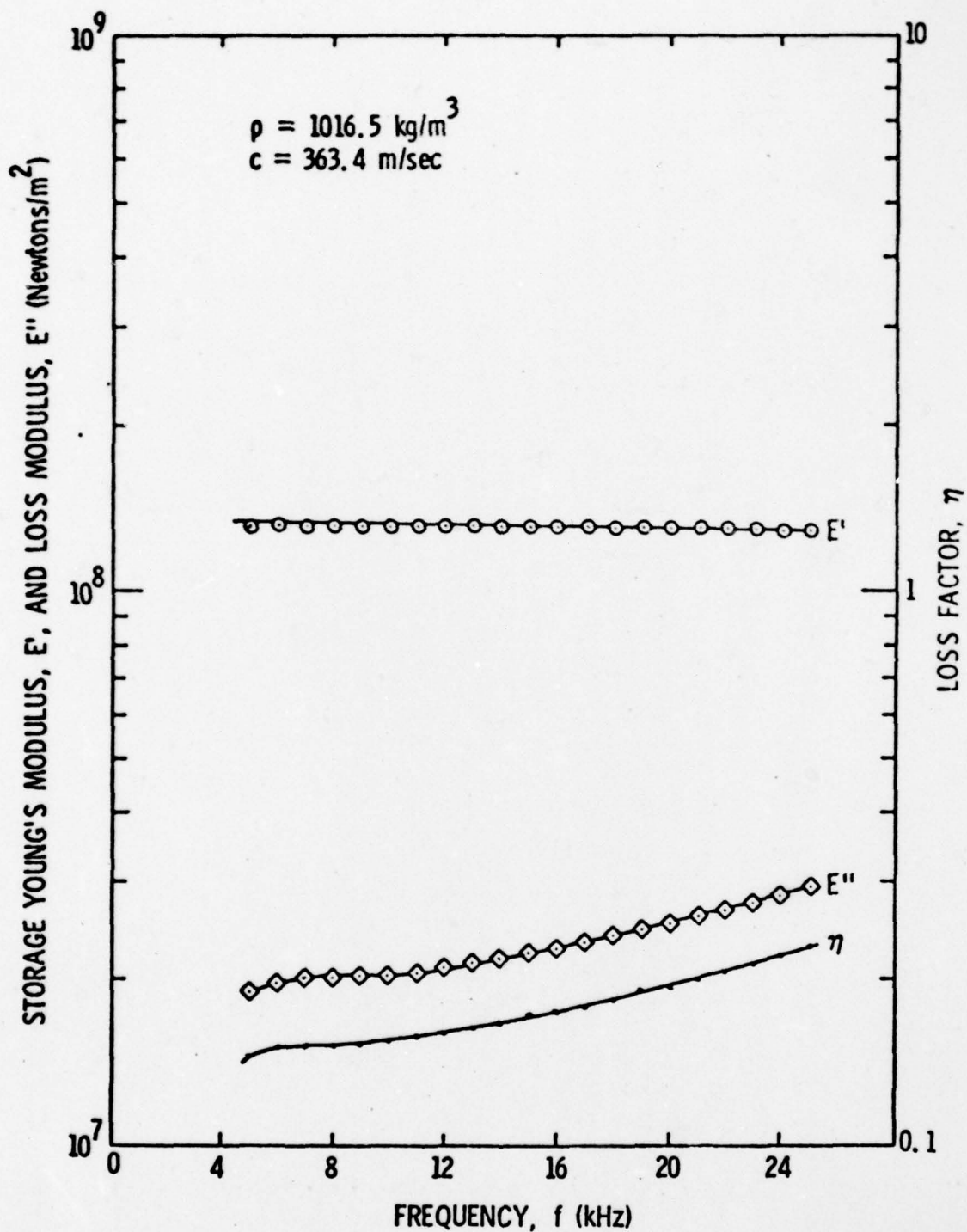


Figure 4.2.4. Storage and Loss Young's Modulus and Loss Factor for EN-6 Polyurethane.

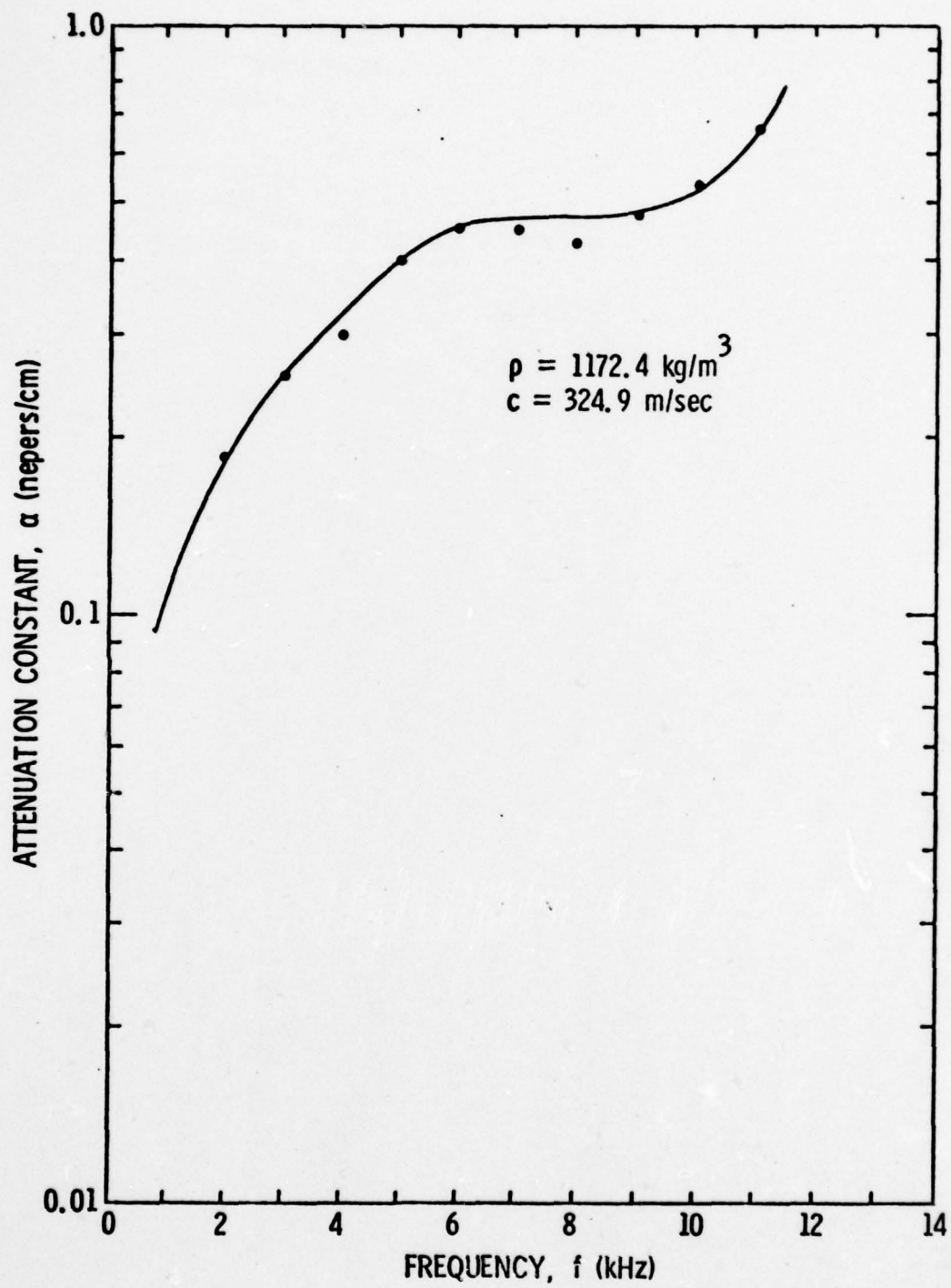


Figure 4.2.5. Attenuation Constant for Hypalon H-862.



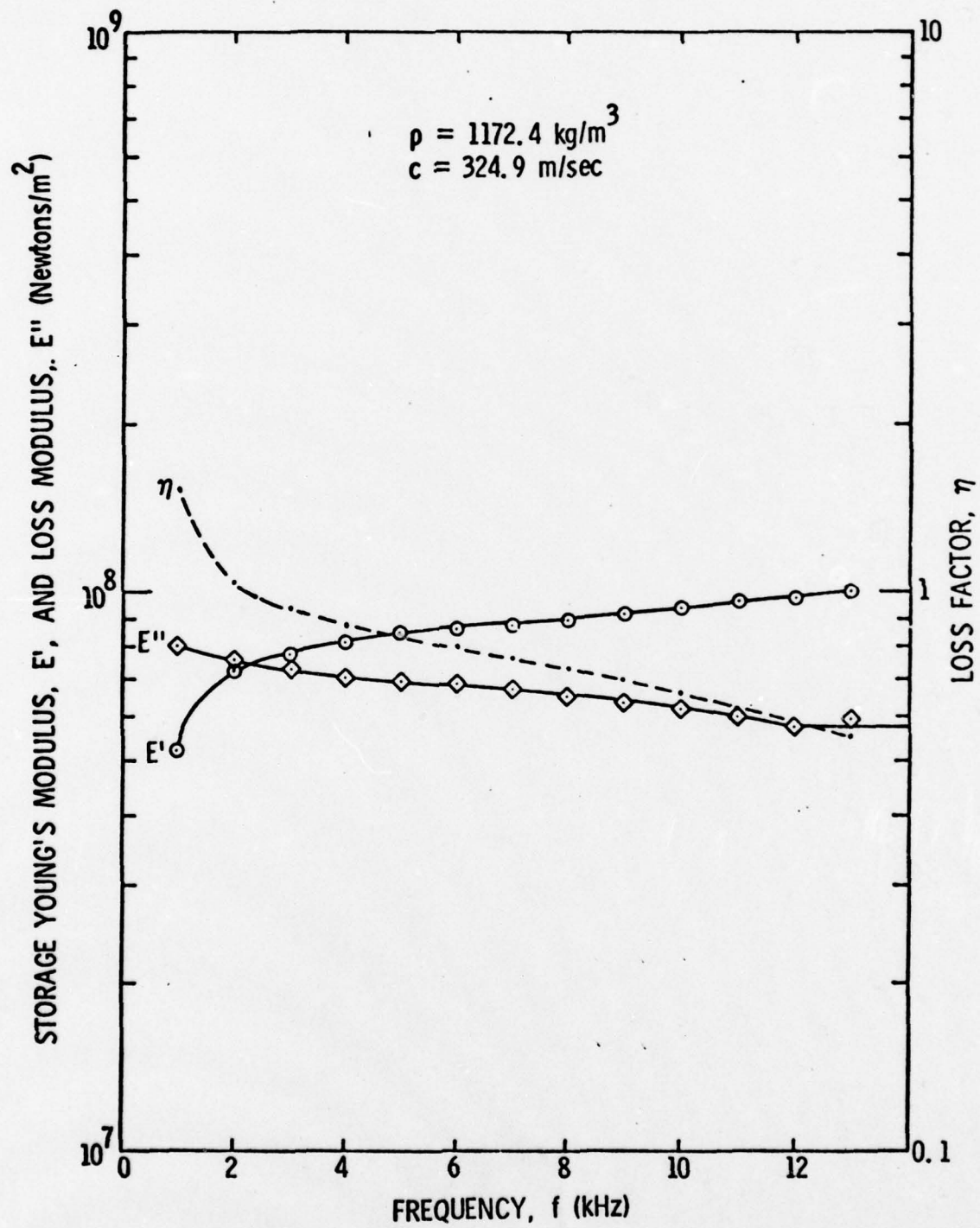


Figure 4.2.6. Storage and Loss Young's Modulus and Loss Factor for Hypalon II-862.

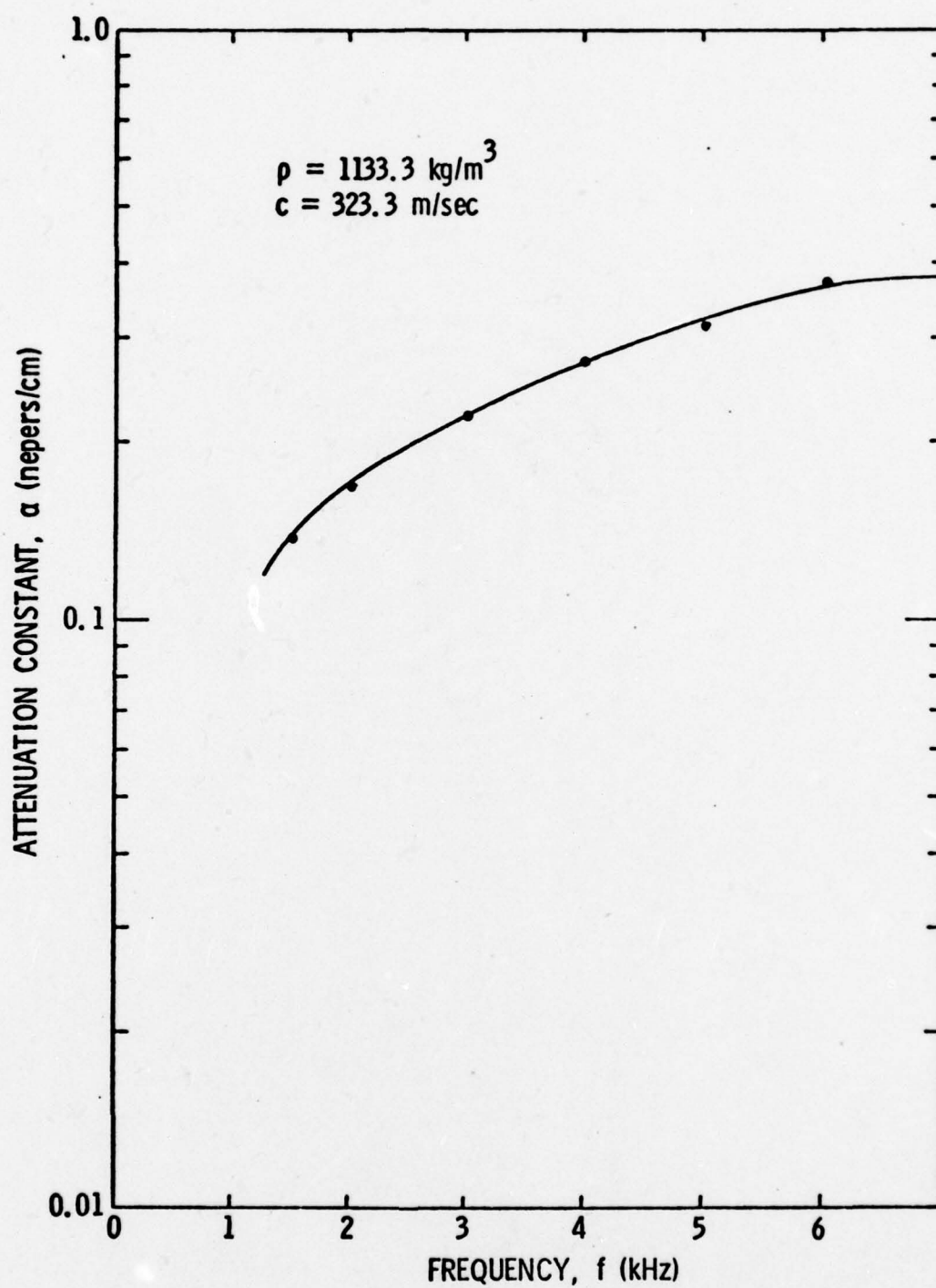


Figure 4.2.7. Attenuation Constant for PRC-1564.

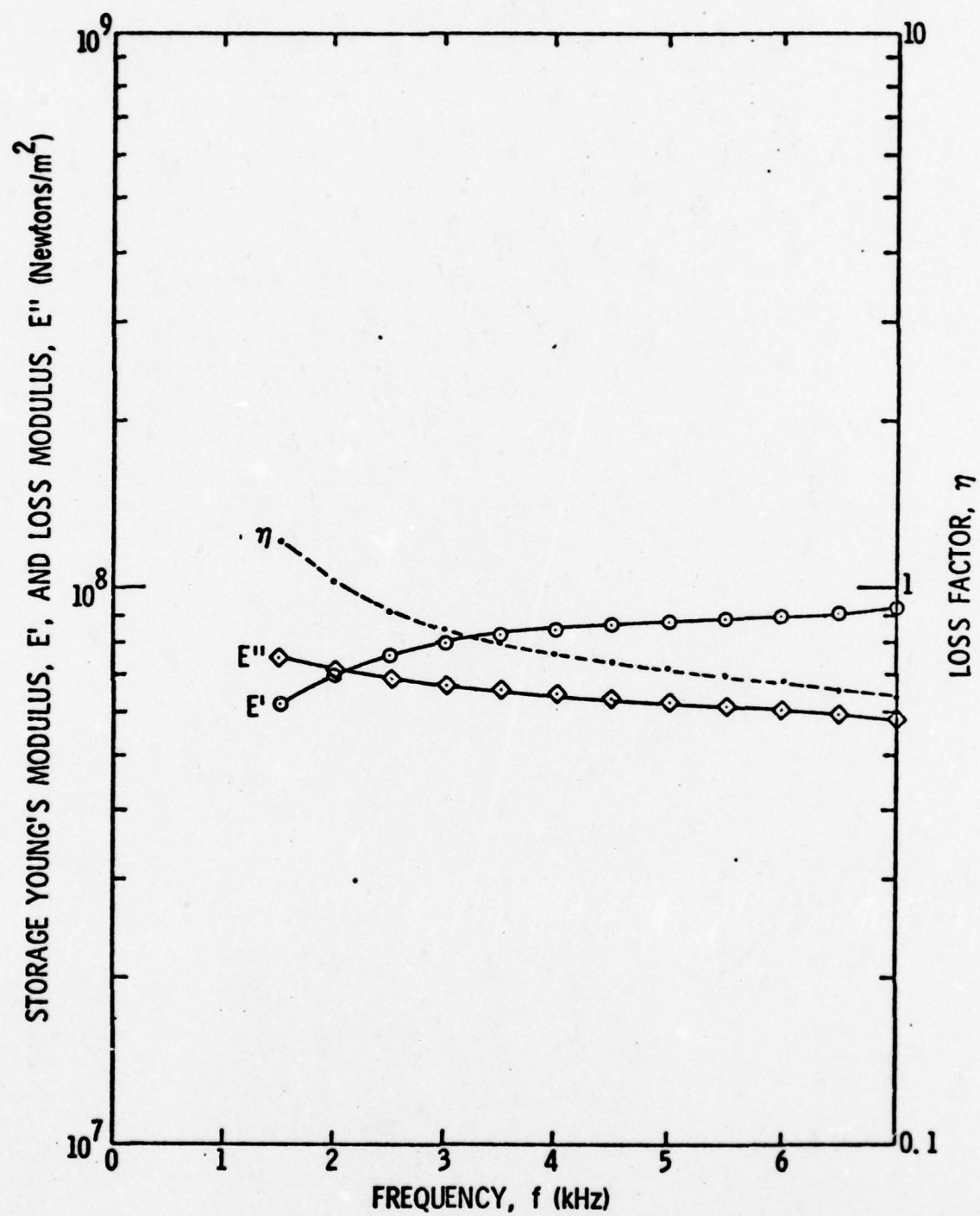


Figure 4.2.8. Storage and Loss Young's Modulus and Loss Factor for PRC-1564.

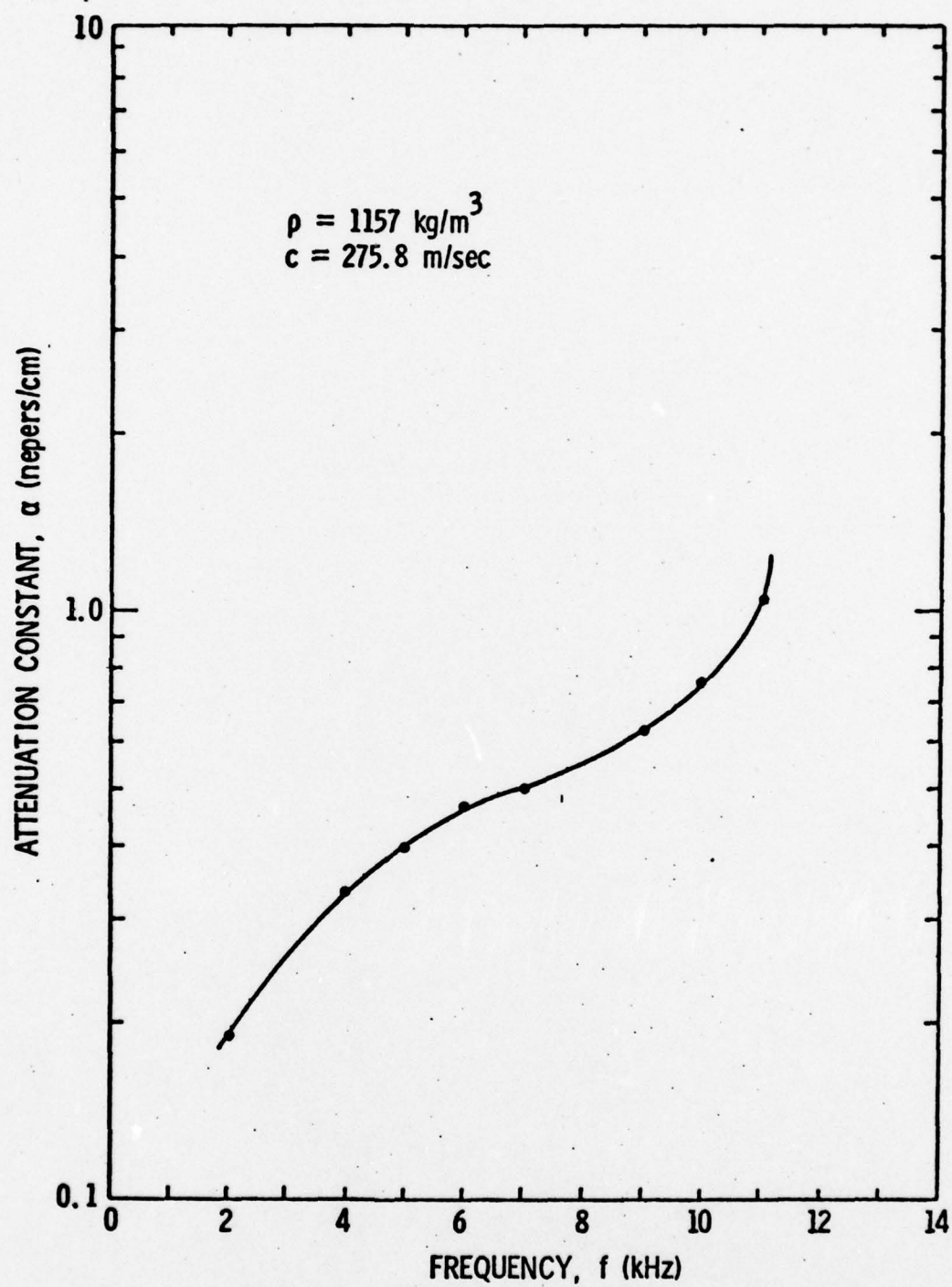


Figure 4.2.9. Attenuation Constant for Butyl B-252.



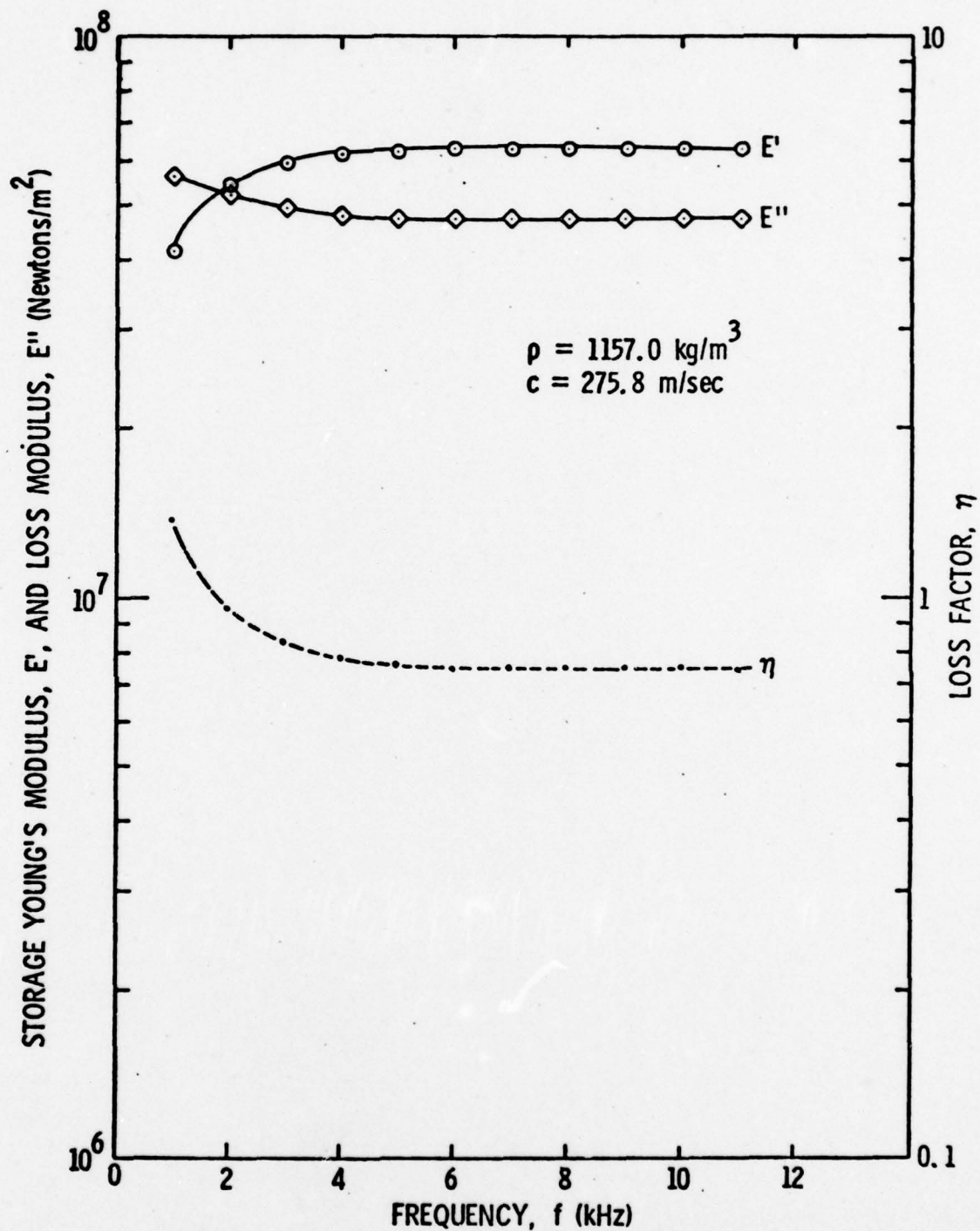


Figure 4.2.10. Storage and Loss Young's Modulus and Loss Factor for Butyl-252.

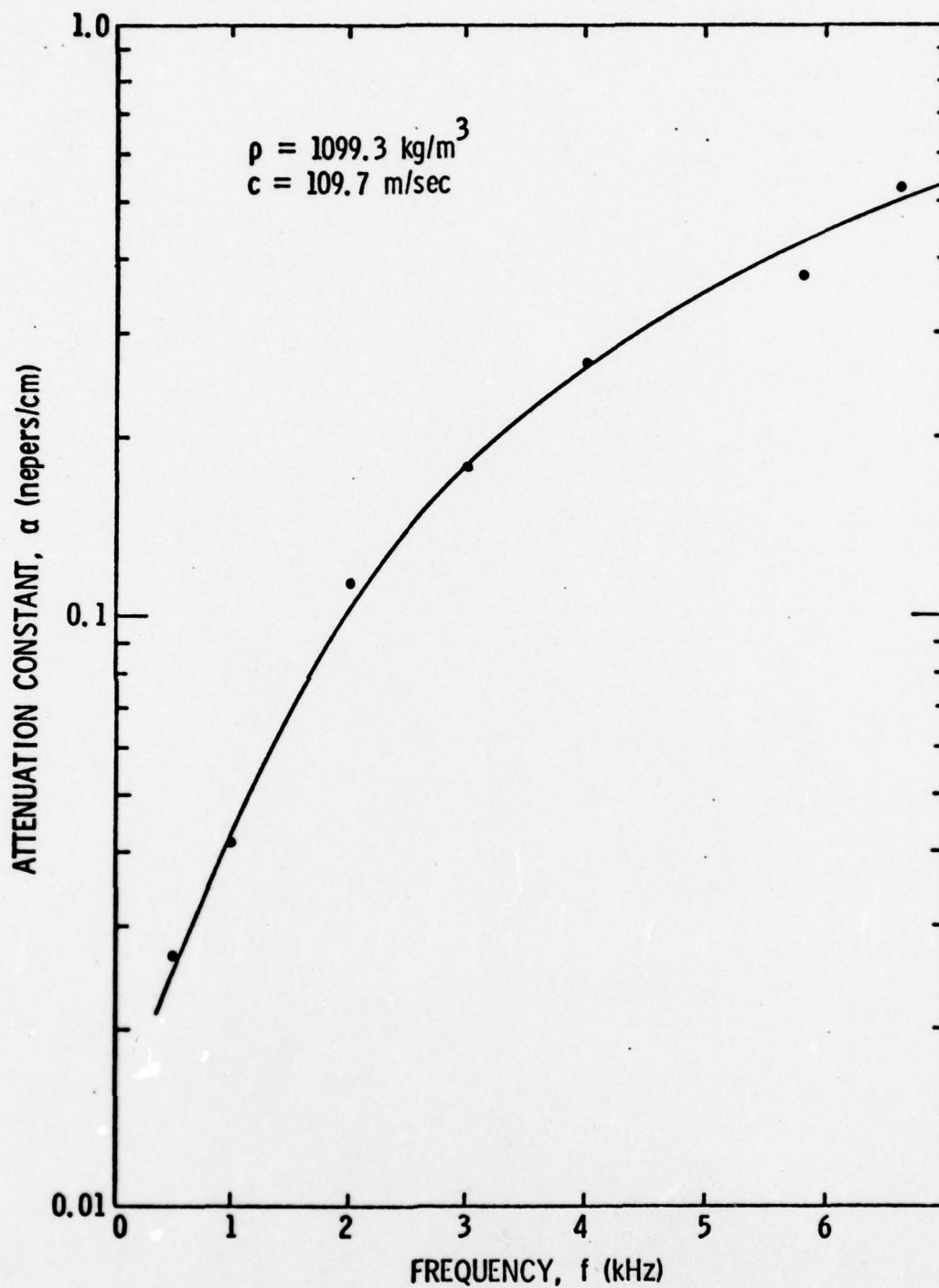


Figure 4.2.11. Attenuation Constant for Natural Rubber 33001.

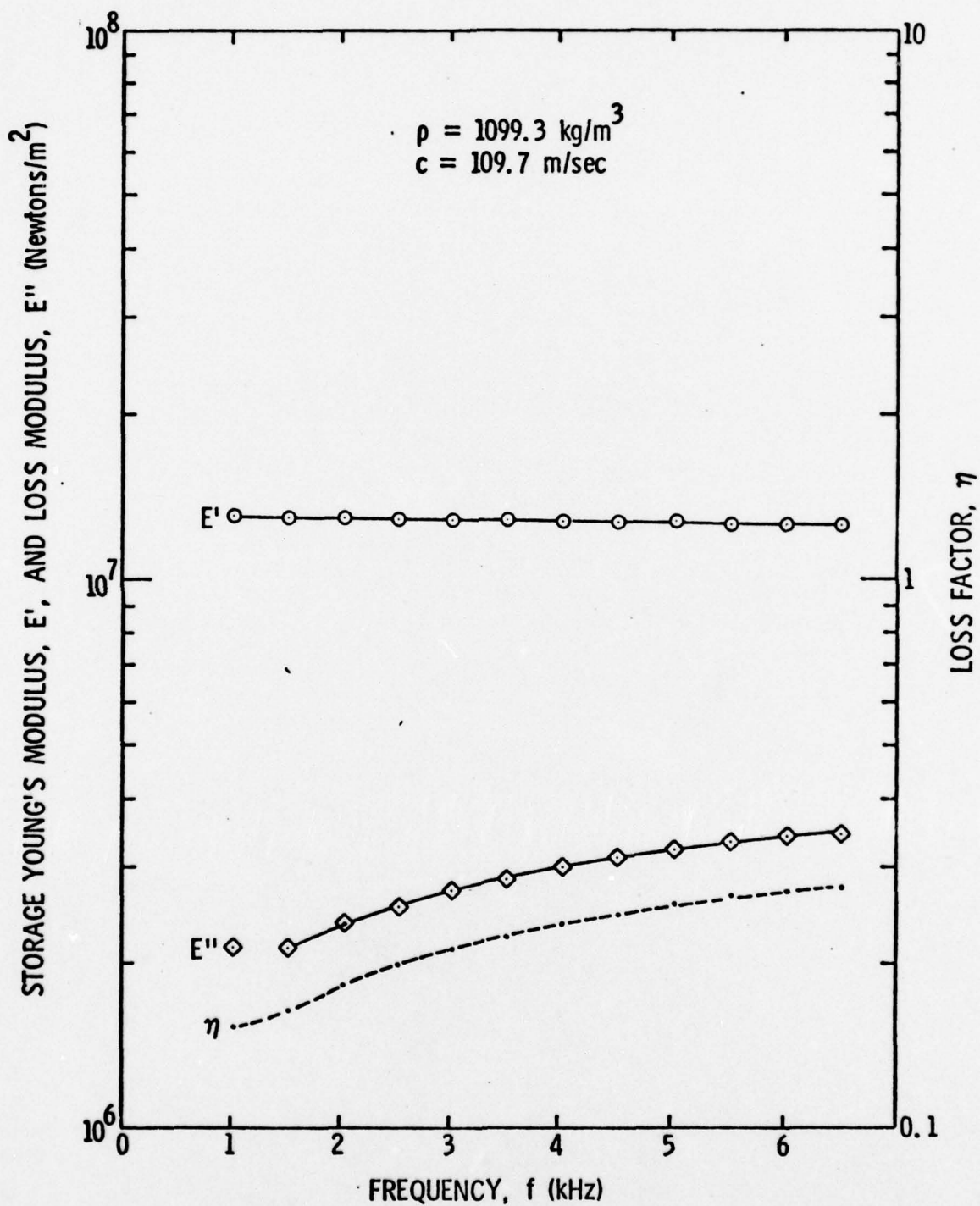


Figure 4.2.12. Storage and Loss Young's Modulus and Loss Factor for Natural Rubber 33001.

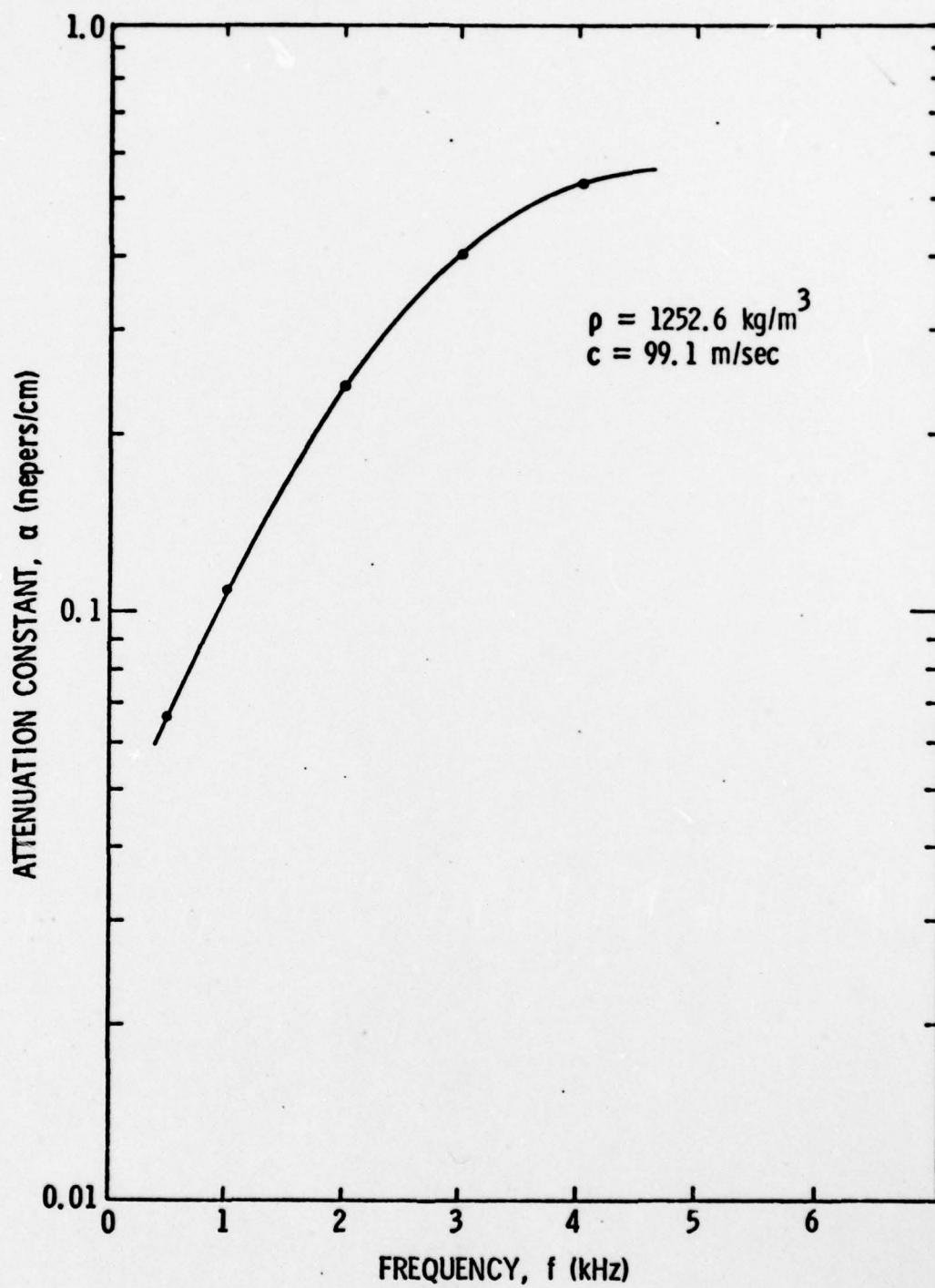


Figure 4.2.13. Attenuation Constant for Neoprene 33003.



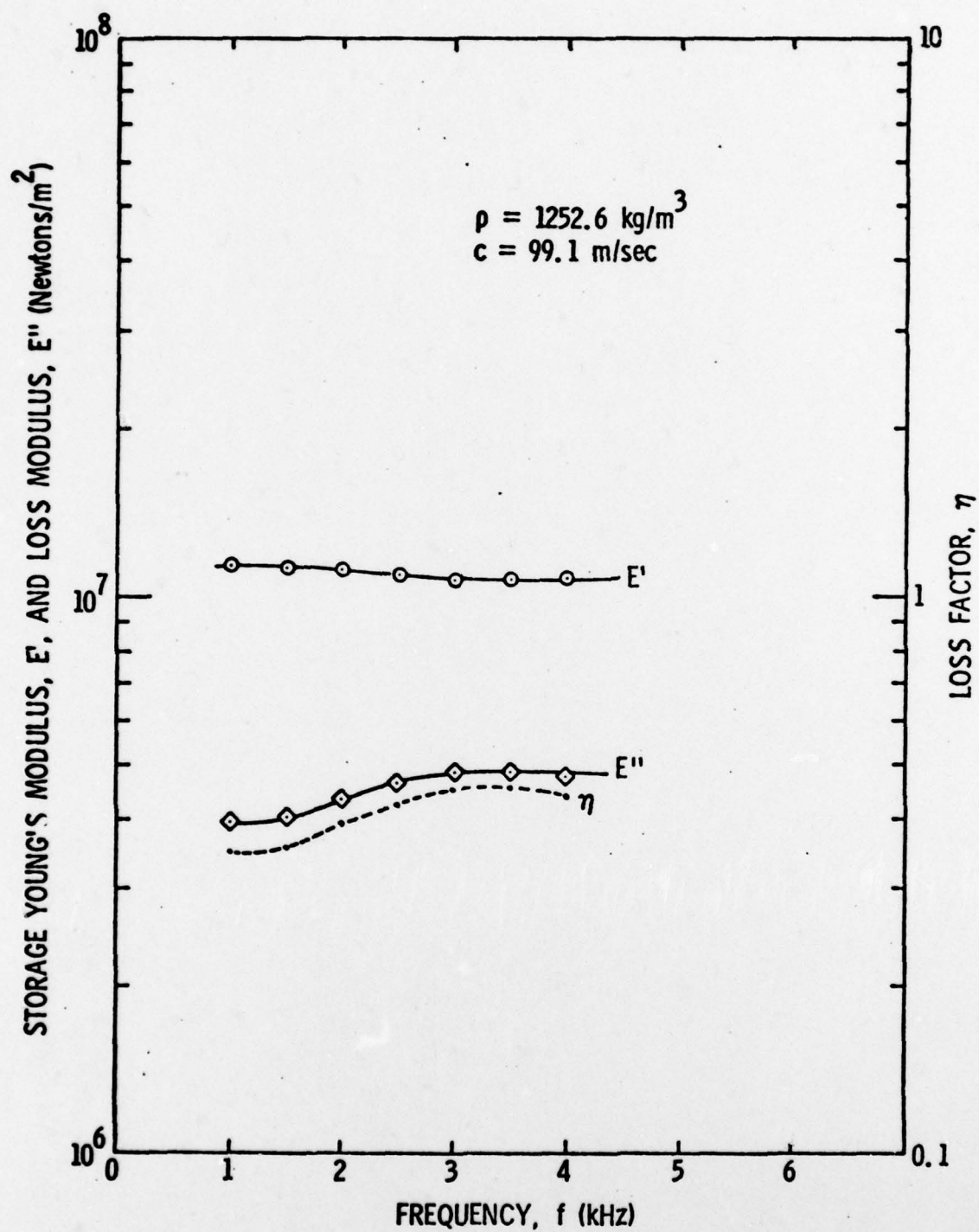


Figure 4.2.14. Storage and Loss Young's Modulus and Loss Factor for Neoprene 33003.

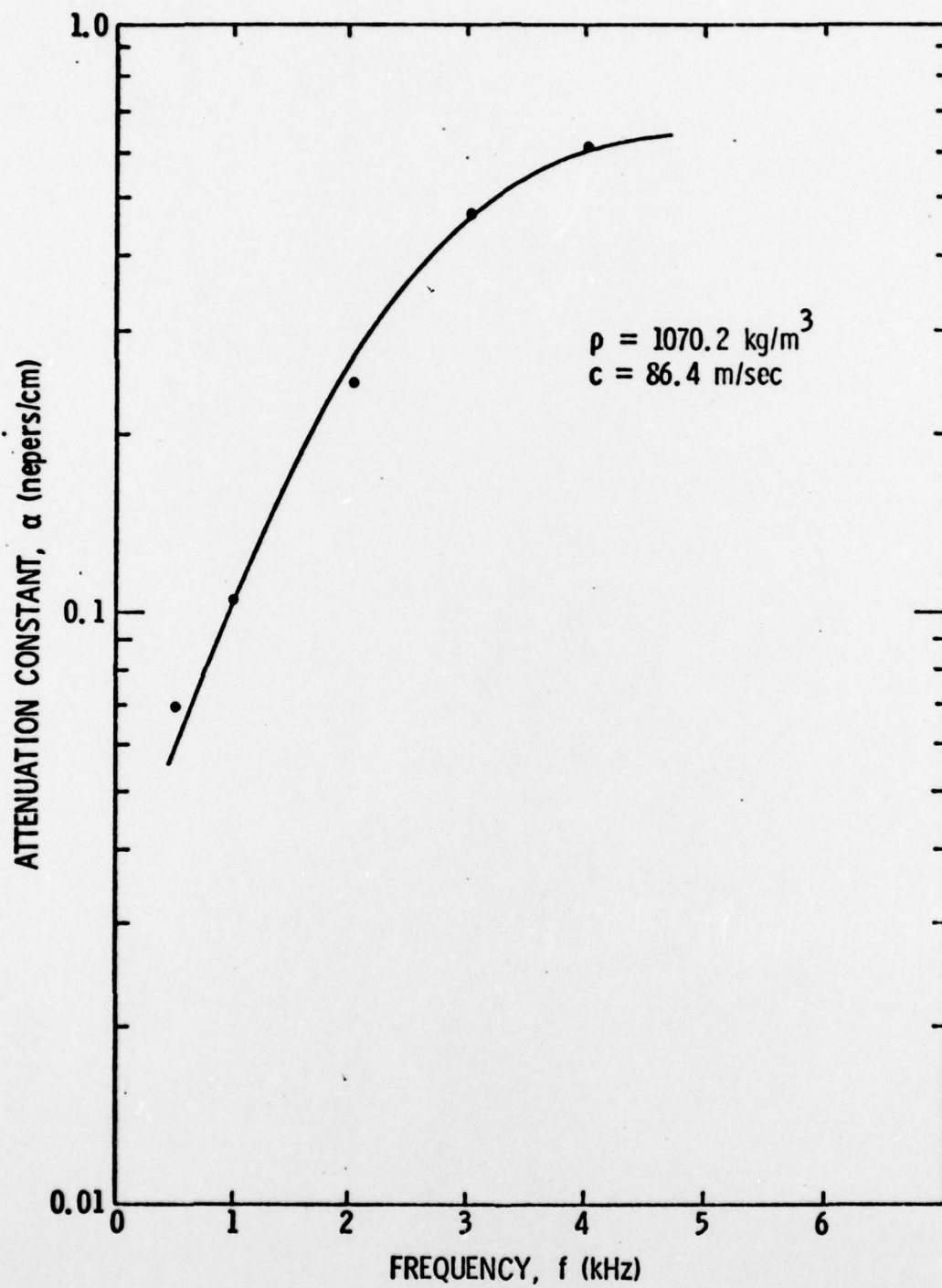


Figure 4.2.15. Attenuation Constant for PRC-1524.

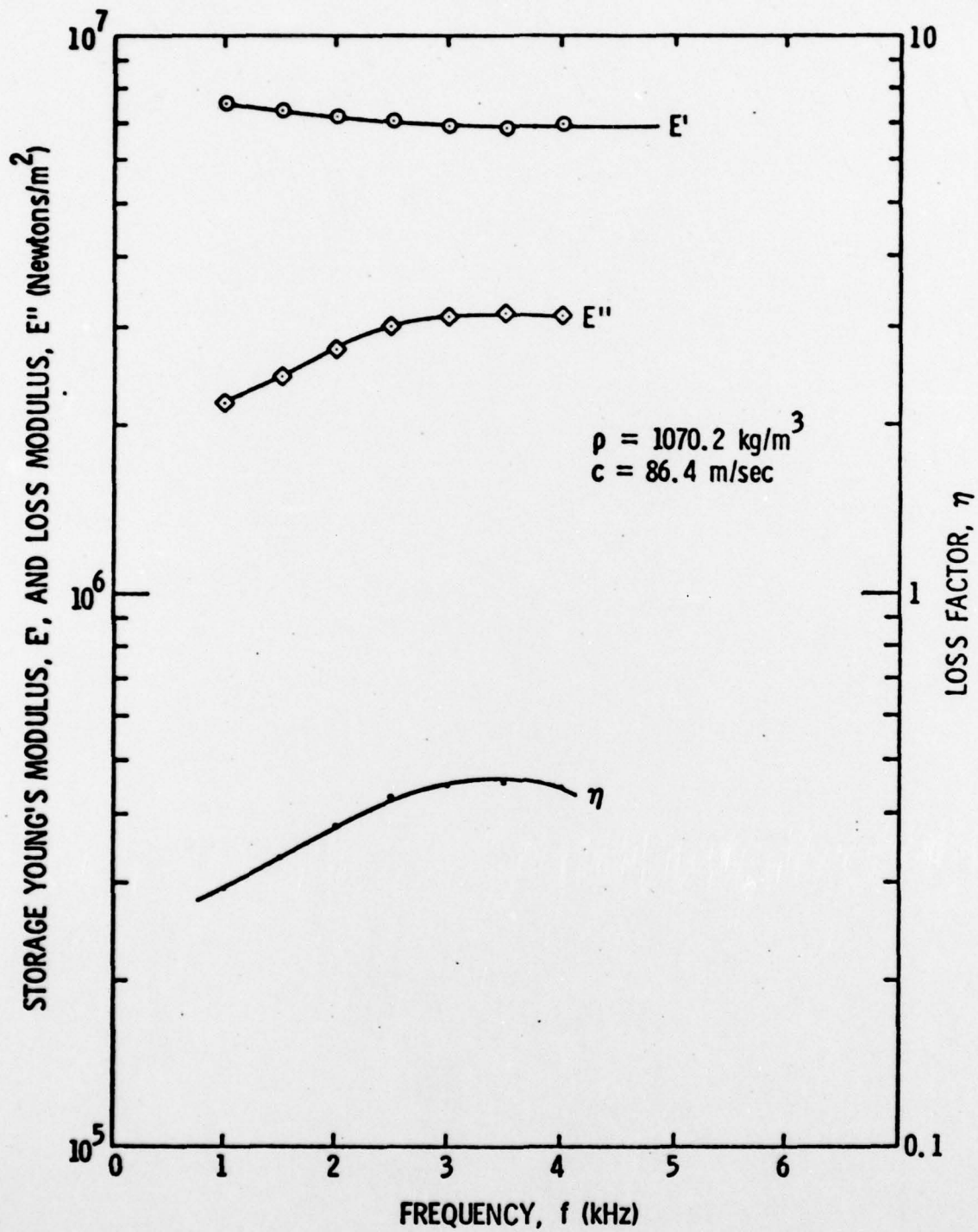


Figure 4.2.16. Storage and Loss Young's Modulus and Loss Factor for PRC-1524.

- (e) Butyl R-252
- (f) Natural Rubber 33001
- (g) Neoprene 33003
- (h) PRC-1524.

These materials are listed from Castomold Polyester which has the highest storage modulus  $E'$  to PRC-1524 with the lowest overall value.

#### 4.3 Error Considerations

The length of the sample (30 cm) made it possible to measure the wavelength and attenuation constant over a considerable distance. Wavelength measurements were more accurate than attenuation measurements, especially at higher frequencies where the signals were attenuated within a few inches in the elastomer. The wavelength could be measured to an estimated precision of  $\pm 4\%$ . The attenuation could be measured with a precision of 6% for the lower frequencies and around 12% for the higher frequencies. The Young's modulus could be measured with a precision of 8%.



## CHAPTER V

### CONCLUSIONS

#### 5.1 Findings

The elastic properties of the eight different materials under observation are summarized in Table 5.1. In Figure 5.1 the variations for the storage modulus are shown graphically; in order to compensate for the large range of frequencies reached with Castomold Polyester and EN-6 Polyurethane and due to the small variation they experience, this figure shows variations up to 12 kHz. It gives an idea of the behavior of all samples. For more detail, the reader is referred to figures in Chapter IV. Figure 5.2 shows the behavior of loss factor for all samples.

#### 5.2 Analysis of Data

It is apparent that in the frequency ranges and temperature at which the materials were tested, they tend to fall into glassy or rubbery region as indicated in Table 5.2.

The storage modulus for glassy materials increases, whereas the loss modulus decreases with frequency. Storage modulus for Castomold Polyester is almost independent of frequency; its loss factor decreases smoothly until 14 kHz, from where it becomes a constant. The storage modulus for Butyl B-252 increases with frequency until 6 kHz, but then, above this frequency, it becomes a constant. At frequencies below 3 kHz, the storage modulus of PRC-1564 is smaller than that of Hypalon H-862, however, at higher frequencies the storage modulus of PRC-1564 becomes larger than that of Hypalon H-862.

Table 5.1. Viscoelastic Properties of Various Elastomers

	Castomold Polyester	EN-6 Polyurethane	Hypalon H-862	PRC-1564
Frequency Range (Hz)	5000 - 25000	5000 - 25000	2000 - 11000	1500 - 7000
Attenuation Constant $\alpha$ (Nepers/cm)	0.037 - 0.11	0.06 - 0.49	0.165 - 0.61	0.14 - 0.4
Storage Modulus $E'$ (Newtons/m <sup>2</sup> )	(1.8 - 1.9) $\times 10^9$	(1.32 - 1.29) $\times 10^8$	(0.73 - 0.97) $\times 10^8$	(0.62 - 0.91) $\times 10^8$
Loss Factor $\eta$	0.3 - 0.18	0.14 - 0.23	1.04 - 0.62	1.2 - 0.64
Loss Modulus $E''$ (Newtons/m <sup>2</sup> )	(0.55 - 0.54) $\times 10^9$	(0.19 - 0.30) $\times 10^8$	(0.76 - 0.61) $\times 10^8$	(0.74 - 0.59) $\times 10^8$
Density $\rho$ (kg/m <sup>3</sup> )	1229.7	1016.5	1172.4	1133.3
Sound Wave Velocity $c$ (m/sec)	1258.9	363.4	324.9	323.3
Characteristic Impedance kg/msec (MKS Rayls)	15.5 $\times 10^5$	3.69 $\times 10^5$	3.81 $\times 10^5$	3.67 $\times 10^5$
Static Young's Modulus $E$ (Newtons/m <sup>2</sup> )	1.95 $\times 10^9$	1.34 $\times 10^8$	1.24 $\times 10^8$	1.18 $\times 10^8$
Region of Viscoelastic Behavior	Glassy	Rubbery	Glassy	Glassy
Figure References	4.2.1 and 4.2.2	4.2.3 and 4.2.4	4.2.5 and 4.2.6	4.2.7 and 4.2.8

Continued

Table 5.1. (Cont.) Viscoelastic Properties of Various Elastomers

	Butyl B-252	Natural Rubber 33001	Neoprene 33003	PRC-1524
Frequency Range (Hz)	1000 - 11000	1000 - 6500	1000 - 4000	1000 - 4000
Attenuation Constant $\alpha$ (Nepers/cm)	0.12 - 0.83	0.04 - 0.5	0.11 - 0.53	0.10 - 0.61
Storage Modulus $E'$ (Newtons/m <sup>2</sup> )	(0.42 - 0.64) $\times 10^8$	(0.13 - 0.125) $\times 10^8$	(0.113 - 0.108) $\times 10^8$	(0.075 - 0.07) $\times 10^8$
Loss Factor $\eta$	1.36 - 0.74	0.15 - 0.27	0.35 - 0.44	0.29 - 0.45
Loss Modulus $E''$ (Newtons/m <sup>2</sup> )	(0.57 - 0.47) $\times 10^8$	(0.021 - 0.034) $\times 10^8$	(0.039 - 0.048) $\times 10^8$	(0.022 - 0.031) $\times 10^8$
Density $\rho$ (kg/m <sup>3</sup> )	1157.0	1099.3	1252.6	1070.2
Sound Wave Velocity $c$ (m/sec)	275.8	109.7	99.1	86.4
Characteristic Impedance kg/msec (MKS Rayls)	$3.19 \times 10^5$	$1.21 \times 10^5$	$1.24 \times 10^5$	$0.925 \times 10^5$
Static Young's Modulus $E$ (Newtons/m <sup>2</sup> )	$0.88 \times 10^8$	$0.13 \times 10^8$	$0.123 \times 10^8$	$0.08 \times 10^8$
Region of Viscoelastic Behavior	Glassy	Rubbery	Rubbery	Rubbery
Figure References	4.2.9 and 4.2.10	4.2.11 and 4.2.12	4.2.13 and 4.2.14	4.2.15 and 4.2.16



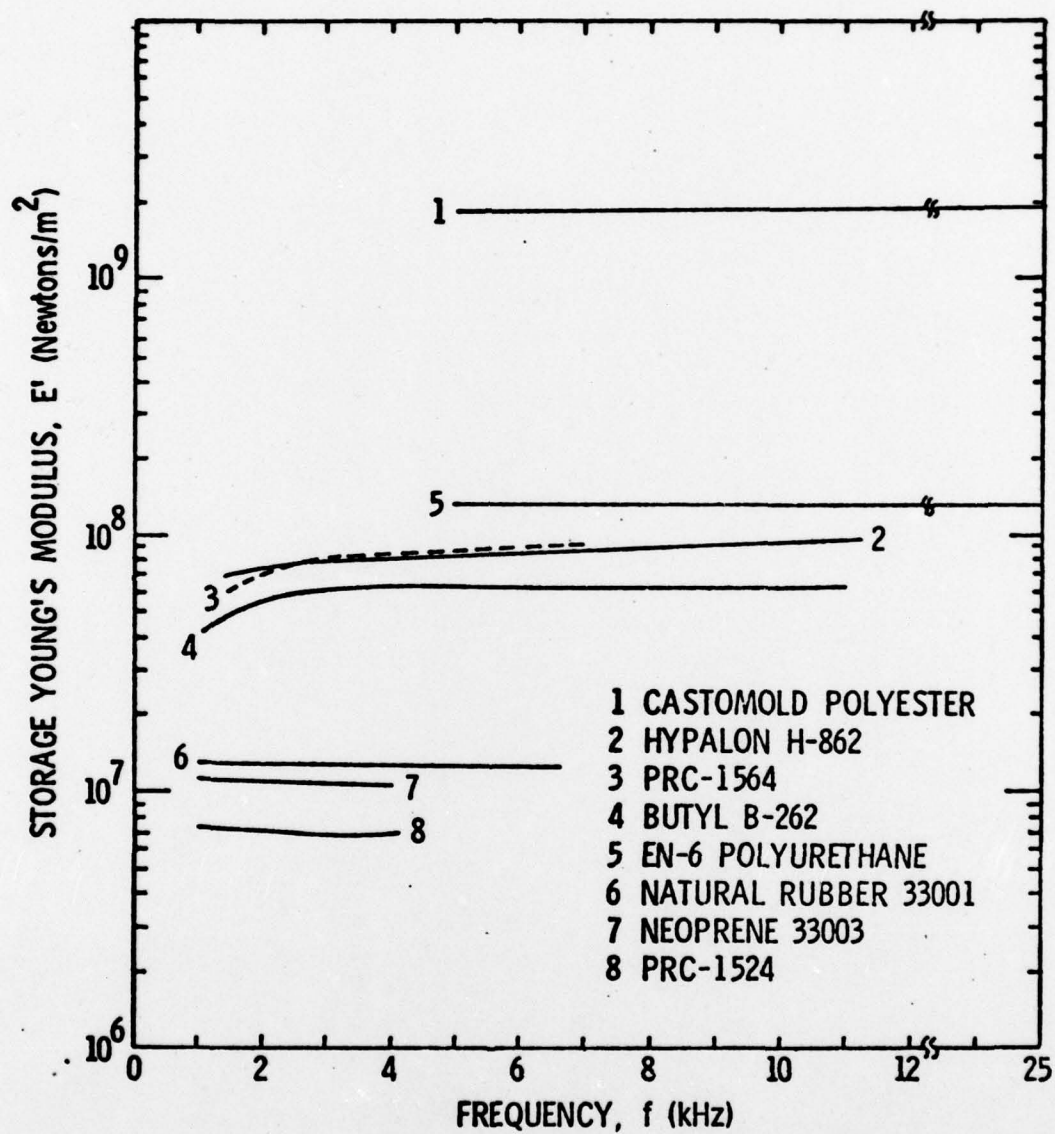


Figure 5.1. Storage Modulus for Eight Viscoelastic Materials.



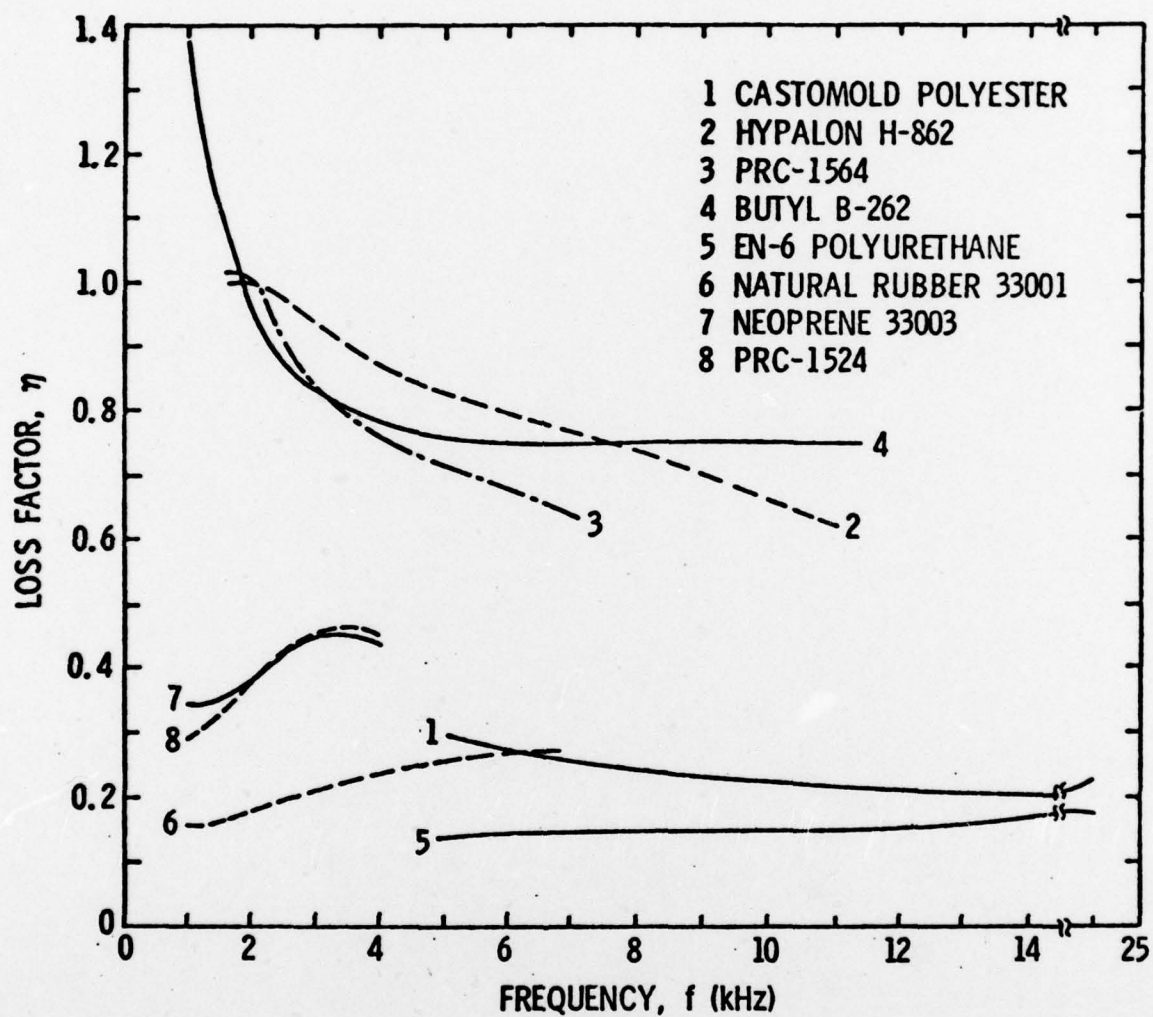


Figure 5.2. Loss Factor for Eight Viscoelastic Materials.

The storage modulus for rubbery materials decreases with frequency, whereas loss modulus increases with it. Storage modulus for Polyurethane depends very little on frequency, its range of frequencies reached is much larger than for the other rubbery materials.

Of these materials, Castomold Polyester has a characteristic impedance of  $15.5 \times 10^5$  MKS Rayls compared to that of water,  $14.8 \times 10^5$  MKS Rayls.

Table 5.2. Categorization of the Tested Materials at 28°C.

<u>Glassy Region</u>	<u>Rubbery Region</u>
1. Castomold Polyester	5. EN-6 Polyurethane
2. Hypalon H-862	6. Natural Rubber 33001
3. PRC-1564	7. Neoprene 33003
4. Butyl B-252	8. PRC-1524

### 5.3 Recommendation for Further Studies

The results of this study show that a stereo cartridge, which can analyze both the longitudinal and transverse waves, can be effectively used in the determination and analysis of viscoelastic properties of elastomers.

In Section 3.6, it was explained how certain technological difficulties made the analysis of transverse waves impossible. In order to overcome these difficulties, further research is recommended. Poisson's ratios (calculated from the data which was obtained for this study) may not agree with the expected values because of the interference due to flexural waves.

Elimination of the unwanted flexural waves will certainly enhance

the accuracy of the calculated values of Poisson's ratio. In order to avoid the flexural wave effect, the use of two cartridges, one on each side of the specimen and at the same distance from the oscillator, is recommended.

## BIBLIOGRAPHY

1. Barnard, G. R., Bardin, J. L. and Whiteley, J. W., "Acoustic Reflections and Transmission Characteristics for Thin Plates," Journal of the Acoustical Society of America, Vol. 57, pp. 577-584 (March 1975).
2. Leaderman, Herbert, "Viscoelastic Phenomena in Amorphous High Polymeric Systems," Chapter I in Rheology - Theory and Applications (F. R. Eirich, ed.) Vol. 2, (Academic Press, New York, 1958).
3. Edwards, A. C. and Farrand, G. N. S., "Elasticity and Dynamic Properties of Rubber," Chapter VIII in The Applied Sciences of Rubber (W. J. S. Naunton, ed.), (Edward Arnold Ltd., London, 1961).
4. Graff, Karl F., Wave Motion in Elastic Solids, (Ohio State University Press, 1975).
5. Blokland, R., Elasticity and Structure of Polyurethane Networks, (Rotterdam University Press, 1968).
6. Snowdon, John C., Vibration and Shock in Damped Mechanical Systems, Chapter I, (John Wiley and Sons Inc., New York, 1968).
7. Bobber, R. J., "Measurements on Auxiliary Materials," Chapter VI in Underwater Electroacoustics Measurements, Naval Research Laboratories (July 1970).
8. Nolle, A. W., "Methods for Measuring Dynamic Mechanical Properties of Rubber-Like Materials," Journal of Applied Physics, Vol. 19, pp. 753-774 (August 1948).
9. Tobolsky, Arthur V., "Stress Relaxation Studies of the Viscoelastic Properties of Polymers," Chapter II in Rheology - Theory and Applications (F. R. Eirich, ed.) Vol. 2, (Academic Press, New York, 1958).
10. Cramer, William S., "Measurements of the Acoustic Properties of Solid Polymers," Naval Ship Research and Development Center, Report 4356 (December 1974).
11. Ferry, J. D., Viscoelastic Properties of Polymers, Chapters IX, X and XI, (John Wiley and Sons Inc., New York, 1970).
12. Kuehl, Walter and Meyer, Erwin, "Dynamic Properties of Rubber and Rubber-Like Substances Over Large Frequency Ranges," Chapter III in Sound Absorption and Sound Absorbers in Water, Naval Ship Report 900,164, Department of the Navy, Bureau of Ships, (Washington, 1947)



13. Nolle, A. W., "Acoustic Determination of the Physical Constants of Rubber-Like Materials," Journal of the Acoustical Society of America, Vol. 19, pp. 194-201 (January 1947).
14. Olson, Harry F., Modern Sound Reproduction, (Van Nostrand Reinhold Co., New York, 1972).
15. Ingard, K. Uno and Morse, Philip M., Theoretical Acoustics, Chapter V, (McGraw Hill Co., New York, 1968).

DISTRIBUTION

Commander (NSEA 09G32)  
Naval Sea Systems Command  
Department of the Navy  
Washington, D. C. 20362

Copies 1 and 2

Commander (NSEA 0342)  
Naval Sea Systems Command  
Department of the Navy  
Washington, D. C. 20362

Copies 3 and 4

Defense Documentation Center  
5010 Duke Street  
Cameron Station  
Alexandria, VA 22314

Copies 5 through 16